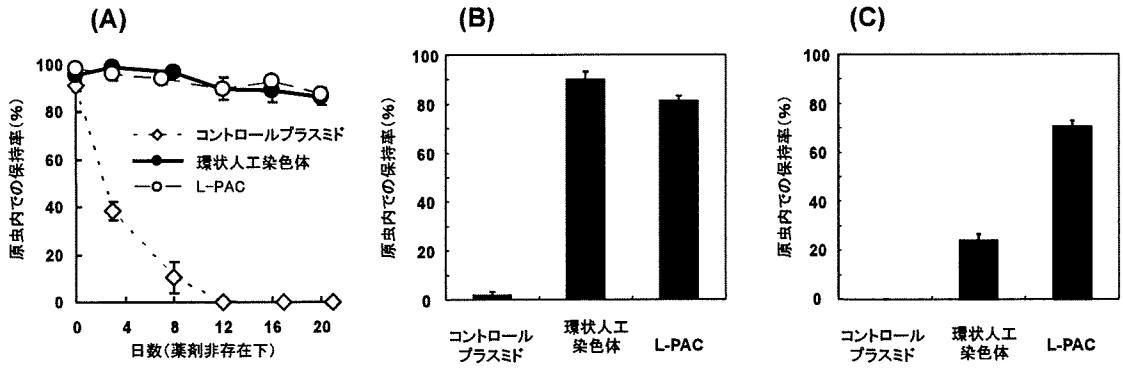

図4 PAC及びセントロメアプラスミドの原虫内での安定性
(A)赤血球ステージの原虫、(B)唾液腺スポロゾイト、(C)肝臓ステージ通過後の赤血球ステージの原虫:原虫内での保持率は全原虫に対するGFP発現原虫の割合(%)より算出した。コントロールプラスミドとしてセントロメア及びテロメアが組み込まれていない環状のプラスミドを使用した。

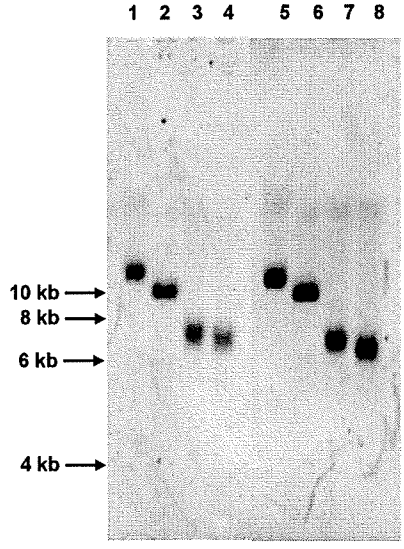

図5 サザンハイブリダイゼーションによるL-PACの制限酵素マッピング
レーン1-4は肝臓ステージ通過後の赤血球ステージの原虫より抽出したゲノムDNA、レーン5-8は薬剤非存在下で20日間維持した赤血球ステージの原虫より抽出したゲノムDNAを使用した。L-PACは原虫ゲノムDNAを抽出した際、同時に回収される。各レーンのゲノムDNAは以下の様に制限酵素処理した。レーン1, 5:未消化、レーン2, 6: *Hind* III消化、レーン3, 7: *Kpn* I 消化、レーン4, 8: *Nhe* I消化。サザンハイブリダイゼーション時にはGFP遺伝子の一部をプローブDNAとして使用した。検出されるDNA断片のサイズは図3に示した。これらの結果を合わせると、PACは直鎖状のまま、原虫内で維持されていることが示される。

Ⅲ. 研究成果の刊行物・別刷

Cell Host & Microbe
Article

p38 MAPK-Dependent Phagocytic Encapsulation Confers Infection Tolerance in *Drosophila*

Naoaki Shinzawa,[1,2] Bryce Nelson,[1] Hiroka Aonuma,[1] Kiyoshi Okado,[1] Shinya Fukumoto,[1] Masayuki Miura,[2] and Hirotaka Kanuka[1,*]
[1]National Research Center for Protozoan Diseases, Obihiro University of Agriculture and Veterinary Medicine, Inada-cho, Obihiro, Hokkaido 080-8555, Japan
[2]Department of Genetics, Graduate School of Pharmaceutical Sciences, University of Tokyo, Bunkyo-ku, Tokyo 113-0033, Japan
*Correspondence: kanuka@obihiro.ac.jp
DOI 10.1016/j.chom.2009.07.010

SUMMARY

Hosts employ a combination of two distinct yet compatible strategies to defend themselves against parasites: resistance, the ability to limit parasite burden, and tolerance, the ability to limit damage caused by a given parasite burden. Animals typically exhibit considerable genetic variation in resistance to a variety of pathogens; however, little is known about whether animals can evolve tolerance. Using a bacterial infection model in *Drosophila*, we uncovered a p38 MAP kinase-mediated mechanism of tolerance to intracellular bacterial infection as measured by the extent to which the host's survival rate increased or was maintained despite increasing bacterial burden. This increased survival was conferred primarily by a tolerance strategy whereby p38-dependent phagocytic encapsulation of bacteria resulted in enlarged phagocytes that trap bacteria. These results suggest that phagocytic responses are not restricted to resistance mechanisms but can also be applied to tolerance strategies for intracellular encapsulation of pathogens during the invertebrate immune response.

INTRODUCTION

Defense against pathogenic microorganisms and other parasites can be divided into two conceptually distinct components: resistance, a character that reduces the pathogen's opportunity of successful infection through an impact on pathogen fitness potentially via pathogen clearance; and tolerance, the host's ability to cope with the impact of a pathogenic encounter without a consequent reduction in fitness to the host (Raberg et al., 2007; Schneider and Ayres, 2008; Corby-Harris et al., 2007; Fornoni et al., 2004). A distinguishing feature between these two strategies for dealing with infection is that resistance has a negative effect on pathogens, whereas tolerance does not, and as a result their relative importance may have substantial consequences for the ecology and evolution of host-pathogen interactions (Rausher, 2001; Roy and Kirchner, 2000). The distinction between resistance and tolerance has attracted considerable attention in studies of the evolution of host defense against pathogens, especially in plants (Fornoni et al., 2004; Rausher, 2001; Roy and Kirchner, 2000), including the idea that hosts generally exhibit genetic variation for both resistance and tolerance (Kover and Schaal, 2002). Despite the many examples that indicate the presence of genetic variation in host fitness postinfection, it is still unclear just how these immune parameters actually relate to host fitness postinfection (Corby-Harris et al., 2007). In fact, many studies have shown that there is not always a positive relationship between immunocompetence parameters and disease resistance, suggesting that host fitness postinfection may also be maintained by a second strategy, namely, infection tolerance. In plants, where tolerance has long been studied, genes conferring disease tolerance have yet to be identified at the molecular level (Raberg et al., 2007; Rausher, 2001). There have been recent reports suggesting a range of tolerance mechanisms in the fruit fly *Drosophila melanogaster* (Ayres et al., 2008; Ayres and Schneider, 2008). *Drosophila* Eiger, an endogenous TNF-α-related ligand, induces a septic shock-like response that damages the fruit fly and subsequently reduces survival rate during *Salmonella* infection (Schneider et al., 2007; Brandt et al., 2004). A recent study using a *foxo* mutant indicates a reduction of insulin signaling and consequent wasting as a primary cause of host lethality in *Mycobacterium*-infected flies (Dionne et al., 2006). In both cases, these intrinsic responses appear to affect tolerance, but not resistance, because changes in these signaling pathways do not alter bacterial burden but do alter survival.

Here we described a function for phagocytic cells in promoting tolerance, but not resistance, in the host defense system. A screen designed to uncover tolerance mechanisma revealed that *Drosophila* p38 mitogen-activated protein (MAP) kinase (Dmp38b), a homolog of the p38 MAP kinase family, mediates host defense response to *S. typhimurium* through phagocytosis-based "packing" of intracellular bacteria into hemocytes without altering bacterial burden. Our results suggest that phagocytic encapsulation contributes to infection tolerance, leading to the sequestration of bacteria and thereby protecting critical host tissues from facing the pathogen.

RESULTS

Dmp38b Mediates Tolerance to *Salmonella* Infection in *Drosophila*

To reveal infection tolerance systems in host defense, we carried out a genetic screen using *Drosophila melanogaster* as an

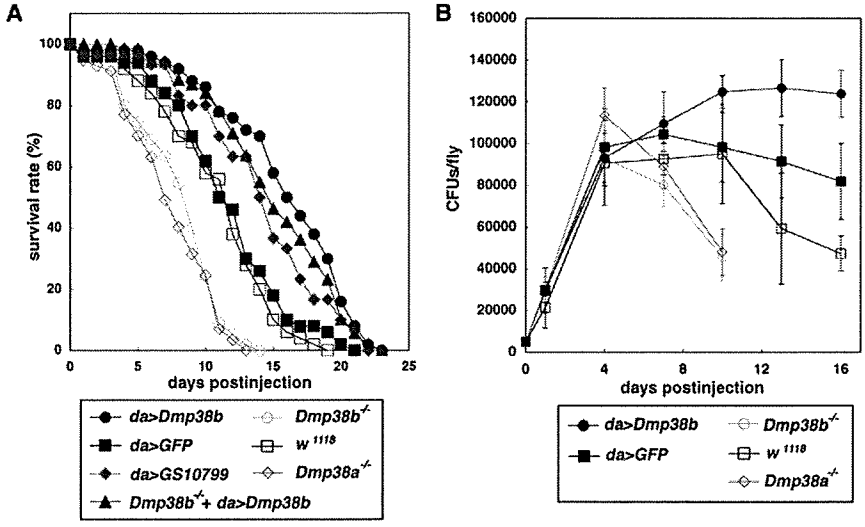

Figure 1. Dmp38b Mediates Infection Tolerance against *Salmonella* Infection in *Drosophila*

The genotypes of flies are as follows: *da > Dmp38b* (*UAS-Dmp38b/Y; da-GAL4/+*); *da > GFP* (*UAS-GFP/+; da-GAL4/+*); *da > GS10799* (*GS10799/+; da-GAL4/+*); *Dmp38b$^{-/-}$+da > GAL4* (*UAS-Dmp38b/Y; Dmp38b$^{-/-}$; da-GAL4/+*).

(A) Survival rates of *Dmp38b*-overexpression flies and null mutant flies were assessed after *Salmonella* (SL1344) infection. $p < 0.05$, comparing *da > GS10799* to *da > GFP*; $p < 0.001$, comparing *da > Dmp38b* and *Dmp38b$^{-/-}$+da > GAL4* to *da > GFP*; $p < 0.001$, comparing *Dmp38b$^{-/-}$* and *Dmp38a$^{-/-}$* to wild-type (*w^{1118}*) (log-rank analysis). This experiment has been performed at least three times.

(B) Bacterial persistence in whole body of *Dmp38b*-overexpression flies and null mutant flies. Bacterial persistence was measured using streptomycin-resistant *Salmonella*. All error bars show standard deviation.

infection model. We focused on the relationship between host survival, thought to be a measure of immunocompetence more directly related to overall host fitness in the presence of infection, and pathogen load within the host, believed to be related to resistance. To identify host factors mediating tolerance, we infected lines of flies expressing a gain-of-function library (Gene Search [GS] System) with the pathogenic bacterium *Salmonella typhimurium* (Toba et al., 1999) and measured host survival rates postinfection before assessing pathogen load in prolonged survival strains (see the Experimental Procedures). No observable decrease in pathogen load in strains with prolonged survival after bacterial infection was taken as an indication of a shift in host defense from resistance to tolerance, a state of coexistence with the invading pathogens. We screened approximately 2869 *Drosophila* GS lines in combination with a ubiquitously expressing GAL4 fly strain (*da-GAL4*), resulting in overexpression of one or two genes from the *Drosophila* genome (Toba et al., 1999). As a result, Dmp38b, one of the *Drosophila* p38 MAP kinases, was identified as a suppressor of *Salmonella*-induced lethality without a subsequent reduction in bacterial load (Figures 1A and 1B and see Figure S1 and Table S1 available online). Conversely, the null mutant for *Dmp38b* showed consistently increased mortality (Figure 1A and Figure S1). No significant difference in bacterial load of *Dmp38b* mutants versus wild-type was observed until day 10, when flies were dying, and therefore we believe it reflects a *Dmp38b*-derived tolerance mechanism rather than resistance mechanisms (Figure 1B). Similar results were obtained from infection with other intracellular bacteria (*Listeria monocytogenes* and *Legionella pneumophila*), but not extracellular bacteria (*Staphylococcus aureus*) (Figure S2), indicating a role within phagocytes for Dmp38b with regards to tolerance during bacterial infection. Furthermore, loss-of-function mutants of Dmp38a, another member of the *Drosophila* p38 MAP kinase family (Craig et al., 2004), exhibited similar phenotypes in the presence of *Salmonella* (Figures 1A and 1B). We attempted to generate a mutant fly deficient for both *Dmp38a* and *Dmp38b*; however, these flies were embryonic lethal (data not shown), suggesting overlapping essential functions for the two p38 MAP kinases during development. Consistent with our observations, *C. elegans* p38 PMK-1 has also been shown to be required for pathogen defense to infection (Kim et al., 2002); therefore the fruit fly might have evolved tolerance-like responses mediated by an evolutionarily conserved function of p38 MAP kinases.

Salmonella Infection Induces Activation of the Dmp38b MAP Kinase Pathway

Drosophila innate immunity can be broadly divided into two categories: humoral and cellular immunity. In order to check whether *Dmp38b* was affecting NF-κB-dependent resistance of flies, aspects of both the humoral and cellular responses were assessed. *Dmp38b* overexpression did not appear to significantly affect induction of antimicrobial peptides (AMPs) (Lemaitre and Hoffmann, 2007; Hoffmann, 2003) or hemocyte-mediated phagocytosis (Elrod-Erickson et al., 2000) (Figures S3A and S3B), consistent with a lack of significant bacterial elimination in adult flies (Figure 1B). This is in contrast to Dmp38a activity in larvae that suppresses AMP expression (Han et al., 1998). Another aspect of resistance involves melanization, a process whose activity can be monitored by measurement of phenoloxidase activity (Soderhall and Cerenius, 1998). Mutation to a melanization-related serine protease (CG3066) affects both resistance and tolerance in a manner highly dependent on the invading pathogen, with resistance to *Salmonella* infection being lowered (Ayres and Schneider, 2008). Interestingly, melanization appeared to be negatively regulated by Dmp38b (Figure S3C). Taken together, it appears that known resistance mechanisms are not responsible for the improved defense against *Salmonella* infection in *Dmp38b*-expressing flies, and therefore the increased survival was likely derived from mechanisms not typically associated with humoral or cellular defenses.

DAP-type peptidoglycan, a cell wall component of Gram-negative bacteria, has been reported to induce *Drosophila* p38-related protein phosphorylation, an activation step required for signal transduction preceding various biological events in vitro (Zhuang et al., 2006). With this in mind, we tested whether

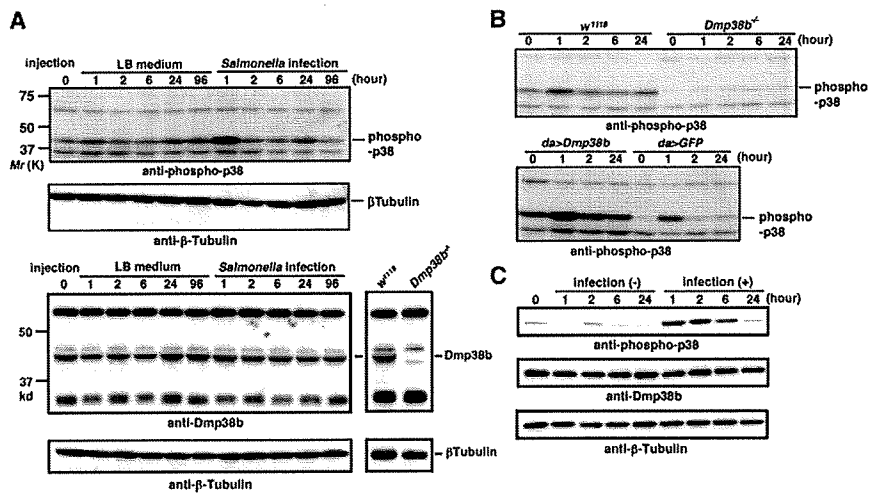

Figure 2. *Salmonella* Infection Induces the Activation of Dmp38b MAP Kinase Pathway

(A) Identification of phosphorylated Dmp38b in *Salmonella*-infected flies. Wild-type flies were injected with bacteria (*Salmonella*) or culture medium (control). The injected flies were collected at indicated time points (hour) and subjected to immunoblotting using anti-phospho-p38 antibody, anti-Dmp38b antibody, and anti-β-tubulin antibody.

(B) Identification of phosphorylated Dmp38b in *Dmp38b*-overexpression and null mutant flies infected with *Salmonella*. The represented strains were collected and subjected to immunoblotting at each indicated time point (hour) after *Salmonella* injection.

(C) Identification of phosphorylated Dmp38b in *Salmonella*-infected S2 cell as a surrogate for adult hemocytes. S2 cells were incubated for 1 hr after *Salmonella* infection, and the lysates were collected and subjected to immunoblotting at each indicated time point (hour).

p38 activation occurred following bacterial challenge in vivo. Rapid induction of p38 phosphorylation was observed within 1 hr post *Salmonella* infection but severely reduced in flies lacking *Dmp38b* (Figures 2A and 2B). In addition, increased amounts of phosphorylated p38 were also observed in response to bacterial invasion in *Dmp38b*-expressing flies. Furthermore, this increase in Dmp38 activity was seen to persist longer than that observed during infection of control flies (Figure 2B, lower panel). Next, p38b activation was examined in *Salmonella*-infected *Drosophila* S2 cells used as a surrogate for adult hemocytes. The phosphorylation of p38b was also detected in the early stages of infection (Figure 2C). It is important to note that this activation of p38b, both in vivo and in vitro, was not an artifact stemming from increased p38b expression (Figures 2A and 2C). Given that phagocytosis occurs within 1 hr postinjection (Figure S3B), it is likely that early encounters between invading bacteria and hemocytes induce the p38 MAPK pathway and contribute to the regulation of tolerance at the earliest stages of infection. Supporting the idea that activation of Dmp38 is required for tolerance to *Salmonella*, null mutants for a MAP kinase kinase kinase dMEKK1, known to be required for peptidoglycan-induced *Drosophila* p38 phosphorylation in vitro (Zhuang et al., 2006), also showed high susceptibility to *Salmonella* infection (data not shown). Taken together, these observations suggest that the *Drosophila* p38 MAP kinase-mediated signaling cascade plays a major role in host tolerance during intracellular bacterial infection in a manner fundamentally different from resistance mechanisms of survival.

Hemocytes Are Responsible Tissue for Dmp38b-Regulated Infection Tolerance

To investigate whether Dmp38b contributes to the in vivo kinetics of *Salmonella* infection tolerance, we observed intracellular proliferation of *Salmonella* using a reporter plasmid (pMIG1), contained within *Salmonella*, that expresses a green fluorescent protein (GFP) only when residing within phagocytic cells (Valdivia and Falkow, 1997). Notably, bacteria were observed persisting and proliferating within phagocytic cells of flies expressing DsRed to mark hemocytes (Brandt et al., 2004) (Figure 3A). Consistent with microscopic observation, bacterial loads in hemolymph from infected flies were found to be approximately 100-fold lower than that seen from whole bodies, suggesting that the majority of *Salmonella* was located inside the hemocytes (the majority of hemocytes in adult flies are attached to structures rather than floating freely within the hemolymph) (Figures 3B and 3C). Inhibition of phagocytic function of hemocytes through introduction of nondigestible latex beads (Elrod-Erickson et al., 2000) significantly enhanced lethality to *Salmonella* infection (Figure 3D), thereby providing further evidence of a role for hemocytes in p38-mediated tolerance. Reciprocally, genetic activation of hemocytes through ectopic expression of *Dmp38b* in hemocytes using a tissue-specific GAL4 driver (*pxn-GAL4*) (Stramer et al., 2005) was sufficient to confer tolerance to levels seen through systemic expression of *Dmp38b* by *da-GAL4* (Figure 3E). Interestingly, despite prolonged survival of flies expressing *Dmp38b* in hemocytes, these hemocytes contained masses of bacteria that outnumbered that seen in control flies (Figures 3B, 3C, 4A, and 4B). It has been observed previously that the general phagocytic capacity (e.g., ability of phagocytosis and/or number of phagocytic cells) of individual wild-type animals was significantly reduced in flies infected with wild-type *Salmonella* (Brandt et al., 2004; Figures S4A and S4B). We therefore tested the phagocytic capacity of *Dmp38b*-expressing flies via hemocyte engulfment of FITC-labeled dead *E. coli* with or without *Salmonella* infection. In stark contrast to control flies infected with *Salmonella*, no significant decrease of phagocytic capacity could be detected in *Dmp38b*-expressing flies (Figures S4A and S4B). However, it is not clear whether the declined phagocytic capacity seen in wild-type *Salmonella*-infected flies is due to hemocyte disruption or phagocytosis impairment and which of these events p38b regulates to maintain phagocytic capacity. Taken together, these results imply that intracellular events in hemocytes are responsible for p38-induced infection tolerance with a resulting persistence of phagocytosis-related capacity in the face of infection.

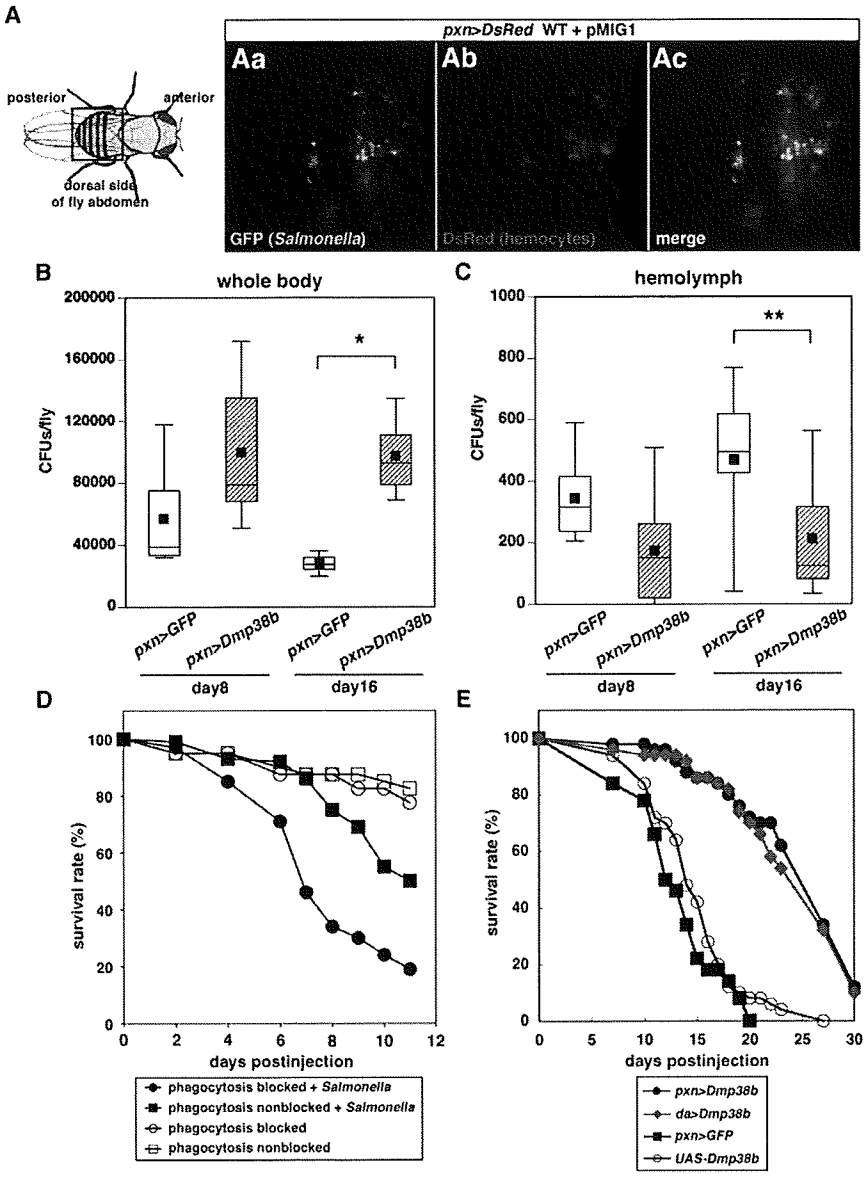

Figure 3. Hemocytes Are Responsible Tissues for Dmp38b-Regulated Infection Tolerance

The genotypes of the flies are as follows: *pxn* > *DsRed* (*pxn-GAL4*; *UAS-DsRed/MKRS, Sb*); *da* > *Dmp38b* (*UAS-Dmp38b/Y*; *da-GAL4/+*); *pxn* > *GFP* (*pxn-GAL4/UAS-GFP*); *pxn* > *Dmp38b* (*UAS-Dmp38b/Y*; *pxn-GAL4/+*); *UAS-Dmp38b* (*UAS-Dmp38b/Y*).

(A) Localization of invading *Salmonella* in plasmatocytes, *Drosophila* macrophage-like phagocytic cells. *pxn* > *DsRed* flies, expressing DsRed in hemocytes, were infected with *Salmonella* containing the phagocytic-inducible GFP reporter (pMIG1). Ectopic fluorescence reveals the colocalization of *Salmonella* (green) with hemocytes (red). Representative images of dorsal area of fly abdomens (shown as black square in schematic image [left panel]) obtained 1 day postinjection of bacteria are shown.

(B and C) Bacterial persistence in whole body (B) and hemolymph (C) in flies with hemocyte-specific overexpression of *Dmp38b* (*pxn* > *Dmp38b*) after *Salmonella* infection. Bacterial persistence was measured using streptomycin-resistant *Salmonella*. Filled square is the median reading, the box extends to the first and third quartiles of the data, and the whiskers indicate the most distant data point that is no more than 2.5 times the interquartile distance from the median. $^{*}p < 0.01$; $^{**}p < 0.05$ (Student's t test).

(D) Survival rates of *Salmonella*-infected flies preinjected with fluorescent latex beads to inhibit phagocytic function of hemocytes. $p < 0.001$, comparing blocked + *Salmonella* to nonblocked + *Salmonella* (log-rank analysis). This experiment has been performed three times.

(E) Survival rate of flies with hemocyte-specific overexpression of *Dmp38b* (*pxn* > *Dmp38b*) after *Salmonella* infection. $p < 0.001$, comparing *da* > *Dmp38b* and *pxn* > *Dmp38b* to *UAS-Dmp38b*; $p < 0.001$, comparing *pxn* > *Dmp38b* to *pxn* > *GFP* (log-rank analysis). This experiment has been performed at least three times.

Persistence of Invaded *Salmonella* in Hemocytes of *Dmp38b*-Overexpression Flies

In order to determine the fate of intracellular bacteria engulfed by p38-overexpressing hemocytes, we carefully observed Dmp38b-modified fruit flies infected with GFP-marked *Salmonella*. The total number of intracellular *Salmonella* within control flies, whose hemocytes had not been incapacitated by infection, clearly decreased during infection (Figures 4Ab and 4Ae), consistent with observations that *Salmonella* invasion into *Drosophila* hemocytes depends upon intact phagocytic cellular processes (data not shown). This is in contrast to hemocyte expression of *Dmp38b* that led to an increase in intracellular persistence of *Salmonella* (Figures 4Aa, 4Ad, and 4B), while reciprocally, loss of *Dmp38b* exacerbated the loss of sustainable phagocytic capacity (Figure 4C). Consistent results were obtained with CFU assays (Figures 3B and 3C). Quantification of fluorescent area derived from GFP-positive intracellular *Salmonella* as an indication of bacterial load indicated that activation of the p38 MAP kinase pathway increased the number of bacteria (Figures 4D–4F), suggesting that bacteria were "packed" into hemocytes. These observations suggest that Dmp38b is involved in the enlargement of hemocytes, thereby enabling large amounts of bacteria to be trapped inside the cell.

Phagocytic Encapsulation Is Required for Dmp38b-Induced Tolerance through Bacterial Sequestration in Hemocytes

To obtain precise mechanistic insights into phagocytosis-linked infection tolerance, we carefully analyzed a confined cluster of *Salmonella* contained within fly phagocytes using a plasmatocyte-specific marker (anti-P1 antibody) (Kurucz et al., 2007). Surprisingly, *Salmonella*-invaded hemocytes had enlarged to an extraordinary size compared to uninfected hemocytes in *Dmp38b*-expressing flies (Figures 5A–5D; Movie S1). Seven

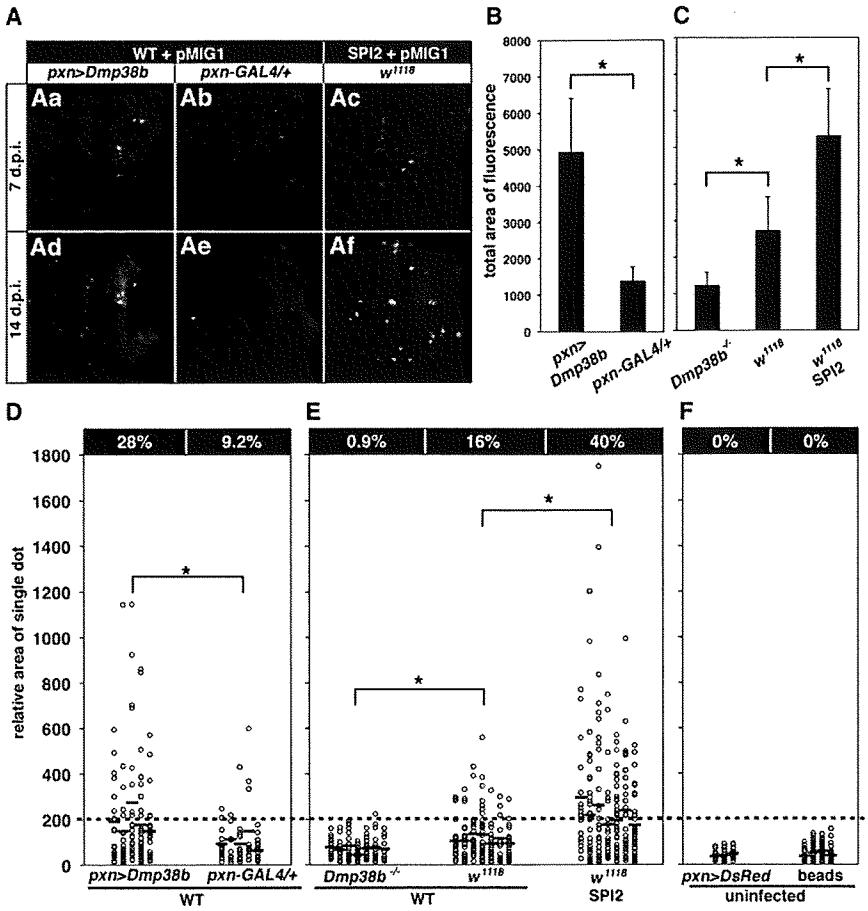

Figure 4. Persistence of Invaded *Salmonella* in Hemocytes of *Dmp38b*-Overexpression Flies

Wild-type *Salmonella* (WT+pMIG1) and SPI-2 mutant *Salmonella* (SPI-2+pMIG1) were used for infection into each line. The genotypes of the flies are as follows: *pxn-GAL4/+* (*+/Y; pxn-GAL4/+*); *pxn > Dmp38b* (*UAS-Dmp38b/Y; pxn-GAL4/+*); *pxn>DsRed* (*pxn-GAL4; UAS-DsRed/MKRS, Sb*).

(A) Ectopic fluorescence image of fly abdomen (at dorsal part, as shown in Figure 3A) represents *Salmonella* persistence in hemocytes (green).

(B and C) Quantification of total area of GFP fluorescence, indicating extent of cellular-invaded *Salmonella* in hemocytes. Each experiment was performed with appropriate genetic background strains. All error bars show standard deviation. *$p < 0.01$ (Student's t test).

(D–F) Quantification of amount of persistent *Salmonella* in each enlarged hemocyte. Wild-type *Salmonella* (WT+pMIG1) and SPI-2 mutant *Salmonella* (SPI-2+pMIG1) were used for infection into each fly strain. The relative fluorescent area in each single GFP dot as shown in (Ad) and (Af) was measured 14 days postinjection. The size of uninfected hemocytes was measured using fluorescent dots in *pxn > DsRed* fly and fluorescent latex bead-injected fly (F). Single marker (open circle) indicates the relative area of one individual fluorescent dot. Each longitudinal plot represents the result obtained from one fly. Blue bar indicates the average. The number in each upper column indicates the percent of enlarged hemocytes (over 200). *$p < 0.0001$ (Student's t test).

days postinfection, invasion of bacteria seemed to induce massive enlargement of hemocytes in both control and *Dmp38b* gain-of-function flies (Figures 5Ea and 5Eb). At the late stages of infection (14 days postinfection), the expansion rate of infected cells appeared to be 3- to 4-fold larger than that of uninfected cells (Figure 5D). Furthermore, it is remarkable that these expanded hemocytes contained huge numbers of *Salmonella*, filling nearly the entire hemocyte (Figure 5Ed). In connection with these observations and considering that the membrane of hemocytes is retained during phagocytic encapsulation, we observed that *Drosophila* p38 MAP kinase expression led to an increase in lamellipodia formation in *Salmonella* infection (Figure S5). We propose that *Drosophila* p38 signaling modulates the remodeling of the actin cytoskeleton in hemocytes that would enable the persistence of enlarged hemocytes and suggest that intracellular packing of pathogens exerts a tolerance mechanism during infection. Supporting the idea that cytoskeleton remodeling modulates phagocytosis-based tolerance, the small GTPase *Drosophila* Rac2 contributes phagocytic defense during *Pseudomonas aeruginosa* infection without affecting AMP expression (Avet-Rochex et al., 2007). We propose the term "phagocytic encapsulation" to describe this phenomenon.

To investigate whether phagocytic encapsulation contributes to fly survival after bacterial infection, we used a nonpathogenic *Salmonella* mutant strain containing a mutation to SPI-2. *Salmonella* contains a *Salmonella* pathogenicity island (SPI) gene cluster encoding a type III secretion system (TTSS); infection of macrophages by *Salmonella* activates the SPI-2 virulence locus that subsequently promotes SPI-2 effectors to act within phagocytic cells to promote intracellular replication and systemic spread (Galan, 2001). SPI-2 mutants can colonize in specific immune tissue (gastrointestinal-associated lymphoid tissue like Payer's patches) but cannot progress to other areas such as mesenteric lymph nodes, suggesting that SPI-2 mutants are unable to proceed past initially invaded cells (Cirillo et al., 1998). As observed previously (Brandt et al., 2004), an SPI-2 mutant deficient for the *ssrA* gene (TM232) and carrying pMIG1 showed little pathogenicity to *Drosophila* and was retained within hemocytes after infection (Figures 4Ac and 4Af and Figure S6). Interestingly, the total number of intracellular *Salmonella* SPI-2 mutants in wild-type flies was comparable to *Dmp38b*-expressing flies (Figures 4A–4C). Furthermore, phagocytic encapsulation of SPI-2 mutants by wild-type hemocytes led to engorgement of hemocytes containing clumps of SPI-2-mutated bacteria (Figures 5Ec and 5Ee; Movie S2) in a manner similar to that seen in *Salmonella*-infected flies expressing *Dmp38b* in hemocytes (Figures 4E–4G). This phagocytic encapsulation was not observed in SPI-2 mutant-infected *Dmp38b* null flies that were found to be sensitive to the SPI-2 pathogenicity (Figure S7). Finally, the p38b-induced tolerant phenotype was abolished when the engulfing function of hemocytes was blocked

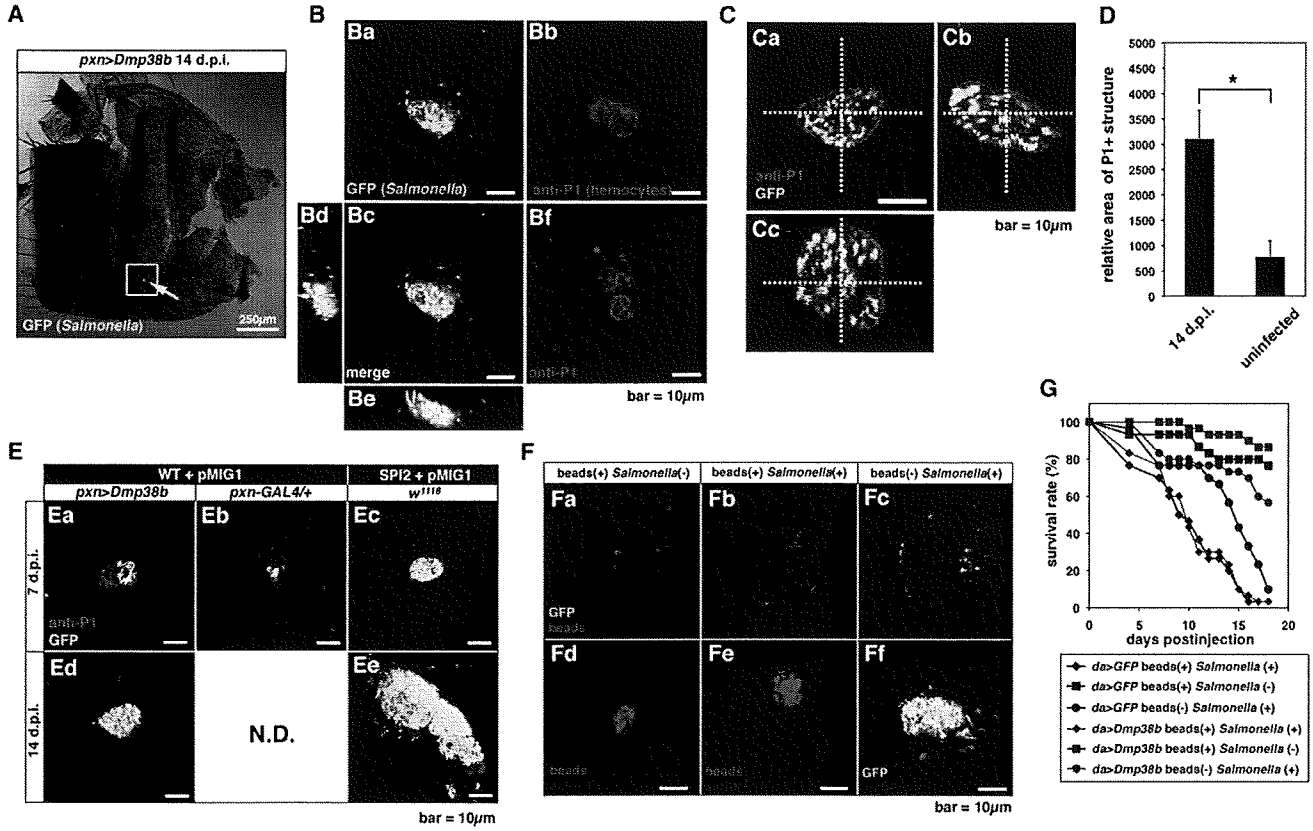

Figure 5. Phagocytic Encapsulation Is Required for p38-Induced Infection Tolerance through Sequestration in Hemocytes

The genotypes of flies used are as follows: *pxn>Dmp38b* (*UAS-Dmp38b/Y; pxn-GAL4/+*); *pxn-GAL4/+* (*+/Y; pxn-GAL4/+*); *da>Dmp38b* (*UAS-Dmp38b/Y; da-GAL4/+*); *da>GFP* (*UAS-GFP/+; da-GAL4/+*).

(A) GFP ectopic fluorescence image of fly abdomen (dorsal part) infected with *Salmonella* (green).

(B) Confined cluster of *Salmonella* encapsulated by plasmatocyte-specific structure shown in high-magnification image of white square region in (A) (Ba–Bc). Note that P1-positive enlarged plasmatocyte (magenta) contains a large number of *Salmonella* (green) (X-Y plain [Bc], Y-Z plain [Bd], and X-Z plain [Be]). Plasmatocytes in uninfected flies are shown in (Bf). Scale bar, 10 μm.

(C) Confocal microscopic image of a confined cluster of *Salmonella* within plasmatocyte specific structure 14 days postinjection. (X-Y plain [Ca], Y-Z plain [Cb], and X-Z plain [Cc]). The three-dimensional image is available as Movie S1. Scale bar, 10 μm.

(D) Relative area of P1-positive plasmatocytes in uninfected and infected (at 14 days postinjection) *Dmp38b*-overexpression flies (*pxn > Dmp38b*). All error bars show standard deviation. *$p < 0.001$ (Student's t test).

(E) Confined cluster of *Salmonella* (green) in plasmatocytes (magenta) in *Dmp38b* gain-of-function flies (*pxn > Dmp38b*) infected with wild-type *Salmonella* (Ea and Ed), wild-type flies (*pxn-GAL4/+*) infected with wild-type *Salmonella* (Eb), and wild-type flies (w^{1118}) infected with SPI-2 mutant *Salmonella* (Ec and Ee). Scale bar, 10 μm.

(F) Blocking of phagocytosis by injection of latex beads inhibits *Salmonella* persistent in hemocytes. Shown are ectopic fluorescence images of fly abdomen (at dorsal part, as shown in Figure 3A) (Fa–Fc) and hemocytes (Fd–Ff). Fluorescent beads (red), P1-stained hemocytes (blue), and *Salmonella* are shown.

(G) Survival rate for *Dmp38b*-overexpressing flies were assessed after *Salmonella* infection with phagocytosis blocking by latex beads injection. $p < 0.01$, comparing *da > Dmp38b* beads (+) *Salmonella* (+) to *da > GFP* beads (+) *Salmonella* (+) (log-rank analysis). This experiment has been performed three times.

in p38b-overexpressing flies through introduction of nondigestible latex beads as well as performed in Figure 3D before infection, suggesting a crucial link between p38b and phagocytic processes (Figures 5F and 5G). This use of phagocyte-blocked flies revealed the remarkable contribution of hemocytes in defense of adult *Drosophila* against systemic infection with *Salmonella* (Defaye et al., 2009). Taken together, these data suggest that p38 MAP kinase-regulated phagocytic encapsulation sequesters and prevents proliferating bacteria from escaping to extracellular areas, thereby providing a mechanism of infection tolerance and enabling the host to suppress the increasing fitness cost resulting from infection.

DISCUSSION

Evolutionary Advantages of an Encapsulation Defense System

Infection tolerance mechanisms confer the ability to limit disease severity induced by a given parasite burden (Raberg et al., 2007; Schneider and Ayres, 2008; Corby-Harris et al., 2007; Fornoni et al., 2004). The work reported here demonstrates an in vivo role for *Drosophila* p38 MAP kinase during bacterial infection through tolerance strategies in the form of phagocytic encapsulation and sequestration in order to defend the host from bacterial virulence. Our present study broadens the concept of

phagocytosis-based immunity by introducing the possibility that phagocytosis is not limited merely to the digestion and autophagy of ingested pathogens but rather might act as a cellular barrier to block pathogen escape. The immune system in vertebrates has evolved the digestion mechanism as a means for antigen presentation, a prerequisite for induction of acquired immunity that is a major strategy to eradicate invaders, and that could conflict with an "encapsulatable" function. However, in the case of invertebrate arthropods lacking an antigen-based acquired immune system, it is likely that greater emphasis would be placed on the isolation and sequestration of engulfed pathogens from a host's vital tissues. Further delineation of the encapsulatable tolerance machinery will provide important insight into primitive immunity as well as host-pathogen interactions.

Pathogen-Sustainable Tolerance Properties in Infected Individuals

Phagocytic encapsulation enables host animals to carry live etiologic agents inside their bodies, thereby potentially providing additional time for eradication or simply acting as a sequestration method to avoid exposure to additional tissues sensitive to pathogenic effects. Furthermore, sequestration of agents capable of triggering immune responses would simultaneously avoid energetically expensive systemic immune responses that can limit life span. Conversely, it is likely that the "packing" event also plays a role in the survival of pathogens themselves. For example, an encapsulation-based cellular response can be exploited for the avoidance from host immune system for years or decades, as represented by *Mycobacterium tuberculosis*-induced latent infection that allows persistence of tubercule bacilli within macrophages in granulomatous lesions (Raupach and Kaufmann, 2001). Thus, phagocytic encapsulation probably contains two conflicting impacts on the host defense system: one whereby conserved tolerance may act as a comprehensive primitive defense system that prevents host animals from suffering damages prior to systemic resistance (e.g., in the case of acquired immunity), and the second in which an indirect effect of tolerance facilitates disease latency in individuals and consequent propagation in animal populations when resistance systems do not fully eliminate invaders.

While this study clearly demonstrates a role for *Dmp38b* in conferring tolerance to flies infected with *Salmonella*, a role for *Dmp38b* in resistance cannot be ruled out. Indeed, survival of an infected organism likely depends on a combination of both resistance to that organism and tolerance to the infection. Such a combination of mechanisms has been proposed to lead to nine different states of an organism (Ayres and Schneider, 2008) ranging from high tolerance coupled with low resistance to low tolerance coupled with high resistance and all states in between. The p38-mediated defense seen in this study potentially falls into the class represented by high tolerance and low resistance. In order to shed light on such complicated defense mechanisms, comprehensive work investigating the synergistic effects of both tolerance and resistance to host fitness will be required.

A provocative finding in this study involves a potential role for *Dmp38b* in the regulation of the melanization cascade, a mechanism involved in infection resistance (Ayres and Schneider, 2008). While previous reports have shown crucial negative regulatory mechanisms for both the Imd and Toll pathways in their regulation of AMP activity (Gordon et al., 2005; Foley and O'Farrell, 2004; Kim et al., 2005; Agaisse and Perrimon, 2004), negative regulation of the melanization cascade remains unclear. Intriguingly, *Dmp38b* appears to act as both a positive regulator for tolerance and a negative regulator of the melanization cascade (Figure S3C). Furthermore, in larvae, *Dmp38a* activity has been associated with a downregulation of AMP activity (Han et al., 1998). A shift from resistance to tolerance would be necessary for long-term survival of an organism, and control of such a shift by a bona fide tolerance mediator would guarantee tight association between these connected survival strategies. Given the conserved role of p38 MAP kinase as a mediator in pathogen-sustainable tolerance systems, our findings may provide a blueprint for host-pathogen interactions that is likely to influence the severity of infectious diseases in other metazoans, including vertebrates.

EXPERIMENTAL PROCEDURES

Fly Strains

Flies were raised on standard *Drosophila* medium at 25°C. *da-GAL4* line, KG01337 line, and other general strains were obtained from Bloomington Stock Center. All GS strains were provided from Kyoto *Drosophila* Genetic Research Center. *UAS-Dmp38b* line was a gift from Takashi Adachi-Yamada (Adachi-Yamada et al., 1999). *pxn-GAL4* line was a gift from Micheal J. Galko (Stramer et al., 2005). *UAS-DsRed* line was a gift from Makoto Sato (Sato and Kornberg, 2002). *Dmp38a* null mutant was a gift from Ross L. Cagan (Craig et al., 2004).

Bacterial Strains and Culture

Salmonella typhimurium (SL1344) and *Listeria monocytogenes* (10403S) were gifts from David Schneider (Brandt et al., 2004; Mansfield et al., 2003). *S. typhimurium* (TM232) was provided by Nobuhiko Okada (Miki et al., 2004). *Legionella pneumophila* (CR39) was provided by Hiroki Nagai (Nagai and Roy, 2001). *Staphylococcus aureus* was provided by Hiroshi Hamamoto and Kazuhisa Sekimizu (Hamamoto et al., 2004). The pMIG1 reporter plasmid was a gift from Stanley Falkow (Valdivia and Falkow, 1997). SL1344 and TM232 were cultured at 37°C in the dark without agitation in LB broth medium with 100 μg/ml streptomycin, and 100 μg/ml streptomycin and 50 μg/ml kanamycin, respectively. For pMIG1 plasmid maintenance, culture medium was supplemented with 100 μg/ml ampicillin. 10403S was cultured at 37°C in the dark without agitation in BHI broth medium with 100 μg/ml streptomycin. CR39 was cultured at 37°C in the dark on charcoal-yeast extract (CYE) plates with 100 μg/ml streptomycin as described previously (Nagai and Roy, 2001), and bacterial patch on the plate were suspended in sterile water for injection. *S. aureus* was cultured at 37°C in the dark with agitation in LB broth medium.

Microbial Infection to Fly and Cells

Seven- to ten-day-old male flies were used for all experiments. Before injection, the bacteria-containing medium was adjusted to appropriate concentration using Gene Quant *pro* (Amersham) with culture medium (SL1344, TM232, and CR39, 0.1 OD; 10403S, 0.01 OD; and *S. aureus*, 0.001 OD). Flies were anesthetized with CO_2 and injected with each strain of bacteria in 65 nl of medium. Injection was carried out by using an individually calibrated pulled glass needle attached to IM-300 microinjector (Narishige). Flies were always injected in the abdomen, close to the junction with thorax and just ventral to the junction between the ventral and dorsal cuticles. After injection, flies were transferred to fresh vials once a week. For inhibition of phagocytosis activity of hemocyte, FluoSpheres red fluorescent (F8763, Invitrogen) were injected into fly as previously described (Elrod-Erickson et al., 2000). For infection to cells, *Drosophila* S2 cells were cultured as previously described (Kanuka et al., 2005). Cells were incubated with bacteria for 1 hr at moi = 10 and treated with 100 μg/ml gentamycin for 1 hr to eliminate unengulfed bacteria.

Gain-of-Function Screening

To identify genes enhancing infection tolerance for bacterial pathogenicity we adapted the *P*-element-based Gene Search (GS) System (Toba et al., 1999). The GS vector contains the UAS enhancer adjacent to a core promoter. In this screen, genes are detected on the basis of phenotypic changes caused by the GAL4-dependent forced expression of the vector-flanking DNA. This system has greater efficiency than others that are presently used for gain-of-function screens (Toba et al., 1999). For the first screen, females of the w^{1118}; +/+; *da-GAL4* genotype were crossed to males from each line in the GS collection. F1 progeny were injected with *Salmonella* (approximately 5000 CFU), and survival rates were monitored daily. The infection phenotypes of GS lines (longer-lived and shorter-lived) were categorized into "suppressor" and "enhancer" of *Salmonella*-induced lethality, respectively. Genomic DNA regions flanking P element of the GS vector were recovered from these GS lines by standard inverse PCR protocols (http://www.fruitfly.org/about/methods/inverse.pcr.html). The recovered genomic fragments were sequenced and analyzed with BLAST at National Center for Biotechnology Information (NCBI) (http://www.ncbi.nlm.nih.gov/blast/Blast.cgi) databases to identify the candidate genes (Table S1). In a secondary screen, bacterial load in each GS line identified as a "suppressor" strain was measured. Strains exhibiting both prolonged survival and normal bacterial load were kept and reexamined for reproducibility of phenotypes.

Dmp38b Mutant Fly

KG01337 (#14364) flies were crossed to transposase-expressing lines (w^{1118}; *Dr/TMS, Sb P*[ry^{+}, $\Delta 2-3$]), and male progeny carrying both elements were mated to w^{1118}; *Tft/CyO* females. Progeny with white eyes were collected and analyzed. Excision lines were screened by genomic PCR and sequenced using sets of primers that recognize genomic sequences flanking the *Dmp38b* locus. An imprecise excised line ($p38b^{ex9}$) was a null mutant line of *Dmp38b*, because RT-PCR analysis revealed that the amount of mRNA for *Dmp38b* was not confirmed in this strain (data not shown). Overexpression of *Dmp38b* rescued the null mutants phenotypes demonstrated in this report (data not shown). RT-PCR was carried out with the following primers sets: *Dmp38b*, 5′-CCGAGAGATCAATGTTGAGGCCGCGAAGTG-3′ and 5′-TTATGTTGTTCA GATCGGCGTCCATCAAGT-3′.

Colony-Forming Assay

Infected flies incubated for indicated durations were homogenized in 10 mM $MgSO_4$ solution, and the diluted series of the homogenized samples were prepared and plated on media containing 100 μg/ml streptomycin for whole-body CFU counts. For hemolymph CFU counts, *Salmonella*-infected flies incubated for indicated durations were injected with 260 nl PBS incubated 10 min before hemolymph was drawn, added to 100 μl 10 mM $MgSO_4$ solution, and plated on media containing 100 μg/ml streptomycin. The CFU in hemolymph was estimated supposing the hemolymph volume of individual flies is 200 nl.

Immunoblotting

For the detection of proteins, infected flies and S2 cells were collected and lysed in SDS sample buffer at each indicated time point. Immunoblotting was performed described previously (Kanuka et al., 2005), using a rabbit anti-active p38 antibody (1:1000, Cell Signaling Technology), rabbit anti-Dmp38b antibody (1:1000, Adachi-Yamada et al., 1999), mouse anti-β-tubulin (1:1000, Chemicon), anti-mouse IgG-HRP antibody (1:2000, Promega), and anti-rabbit IgG-HRP (1:2000, Cell Signaling Tchnology). The signals were visualized using Immobilon Western kit (Millipore). Immunoblotting of anti-β-tubulin antibody was used as a loading control.

Immunohistochemistry

Immunostaining of abdominal regions was carried out as previously reported (Kanuka et al., 2005) with some modification. The following antibodies and fluorescent materials were used for immunostaining: mouse P1 monoclonal antibody (1:10, a gift from Dr. Istvan Ando) (Kurucz et al., 2007), goat anti-mouse IgG-Alexa 568 (1:100, Invitrogen), goat anti-mouse IgG-Alexa 488 (1:100, Invitrogen), and FluoSpheres red fluorescent (F8763, Invitrogen). To analyze the topology of the infected hemocytes, optical sections were obtained along the z axis at 0.2 μm intervals, and the images of the X-Z and Y-Z planes were reconstructed by using Leica AF software (Leica). For quantitative analysis of fluorescence in the dorsal side of the abdomen, legs and wings were removed from anesthetized fly bodies and fixed on glass slides with double-sided adhesive tape. All fluorescent signals were examined using a MZ 16F fluorescence microscope for fly image and a TCS SP5 confocal microscopy for plasmatocytes image (Leica). Quantification of represented images was assessed by using ImageJ software (National Institutes of Health [NIH]).

SUPPLEMENTAL DATA

Supplemental Data include Supplemental Experimental Procedures, one table, seven figures, Supplemental References, and two movies and can be found with this article online at http://www.cell.com/cell-host-microbe/supplemental/S1931-3128(09)00258-3.

ACKNOWLEDGMENTS

We are grateful to T. Adachi-Yamada, Y. Matsumoto, T. Aigaki, M. Sato, M. Galko, R. Cagan, Kyoto *Drosophila* Genetic Research Center, and Bloomington Stock Center for fly strains; D.S. Schneider, S. Falkow, N. Okada, H. Nagai, H. Hamamoto, and K. Sekimizu for bacterial strains and plasmids; S. Kawabata for a reagent; and I. Ando for antibodies. We are also grateful to E. Kuranaga, Y. Horiguchi, A. Abe, and K. Kawamoto for valuable discussions. This study was supported in part by grants from Health Sciences Research Grant for Research on Emerging and Re-emerging Infectious Diseases from the Ministry of Health, Labor, and Welfare (to H.K. and S.F.); Grants-in-Aid for Scientific Research from Japanese Ministry of Education, Science, Sports, Culture and Technology (to H.K. and S.F.); Astellas Foundation for Research on Metabolic Disorders (to H.K.); and the Program for the Promotion of Basic Research Activities for Innovative Biosciences (PROBRAIN) (to H.K.). N.S. and B.N. are research fellows of the Japan Society for the Promotion of Science.

Received: February 6, 2009
Revised: May 11, 2009
Accepted: July 27, 2009
Published: September 16, 2009

REFERENCES

Adachi-Yamada, T., Nakamura, M., Irie, K., Tomoyasu, Y., Sano, Y., Mori, E., Goto, S., Ueno, N., Nishida, Y., and Matsumoto, K. (1999). p38 mitogen-activated protein kinase can be involved in transforming growth factor beta superfamily signal transduction in *Drosophila* wing morphogenesis. Mol. Cell. Biol. *19*, 2322–2329.

Agaisse, H., and Perrimon, N. (2004). The roles of JAK/STAT signaling in *Drosophila* immune responses. Immunol. Rev. *198*, 72–82.

Avet-Rochex, A., Perrin, J., Bergeret, E., and Fauvarque, M.O. (2007). Rac2 is a major actor of *Drosophila* resistance to *Pseudomonas aeruginosa* acting in phagocytic cells. Genes Cells *12*, 1193–1204.

Ayres, J.S., and Schneider, D.S. (2008). A signaling protease required for melanization in *Drosophila* affects resistance and tolerance of infections. PLoS Biol. *6*, e305. 10.1371/journal.pbio.0060305.

Ayres, J.S., Freitag, N., and Schneider, D.S. (2008). Identification of *Drosophila* mutants altering defense of and endurance to *Listeria monocytogenes* infection. Genetics *178*, 1807–1815.

Brandt, S.M., Dionne, M.S., Khush, R.S., Pham, L.N., Vigdal, T.J., and Schneider, D.S. (2004). Secreted bacterial effectors and host-produced Eiger/TNF drive death in a *Salmonella*-infected fruit fly. PLoS Biol. *2*, e418. 10.1371/journal.pbio.0020418.

Cirillo, D.M., Valdivia, R.H., Monack, D.M., and Falkow, S. (1998). Macrophage-dependent induction of the *Salmonella* pathogenicity island 2 type III secretion system and its role in intracellular survival. Mol. Microbiol. *30*, 175–188.

Corby-Harris, V., Habel, K.E., Ali, F.G., and Promislow, D.E. (2007). Alternative measures of response to *Pseudomonas aeruginosa* infection in *Drosophila melanogaster*. J. Evol. Biol. *20*, 526–533.

Craig, C.R., Fink, J.L., Yagi, Y., Ip, Y.T., and Cagan, R.L. (2004). A *Drosophila* p38 orthologue is required for environmental stress responses. EMBO Rep. *5*, 1058–1063.

Defaye, A., Evans, I., Crozatier, M., Wood, W., Lemaitre, B., and Leulier, F. (2009). Genetic ablation of *Drosophila* phagocytes reveals their contribution to both development and resistance to bacterial infection. J. Innate Immun. *1*, 322–334.

Dionne, M.S., Pham, L.N., Shirasu-Hiza, M., and Schneider, D.S. (2006). Akt and FOXO dysregulation contribute to infection-induced wasting in *Drosophila*. Curr. Biol. *16*, 1977–1985.

Elrod-Erickson, M., Mishra, S., and Schneider, D. (2000). Interactions between the cellular and humoral immune responses in *Drosophila*. Curr. Biol. *10*, 781–784.

Foley, E., and O'Farrell, P.H. (2004). Functional dissection of an innate immune response by a genome-wide RNAi screen. PLoS Biol. *2*, e203. 10.1371/journal.pbio.0020203.

Fornoni, J., Nunez-Farfan, J., Valverde, P.L., and Rausher, M.D. (2004). Evolution of mixed strategies of plant defense allocation against natural enemies. Evolution Int. J. Org. Evolution *58*, 1685–1695.

Galan, J.E. (2001). Salmonella interactions with host cells: type III secretion at work. Annu. Rev. Cell Dev. Biol. *17*, 53–86.

Gordon, M.D., Dionne, M.S., Schneider, D.S., and Nusse, R. (2005). WntD is a feedback inhibitor of Dorsal/NF-kappaB in *Drosophila* development and immunity. Nature *437*, 746–749.

Hamamoto, H., Kurokawa, K., Kaito, C., Kamura, K., Manitra Razanajatovo, I., Kusuhara, H., Santa, T., and Sekimizu, K. (2004). Quantitative evaluation of the therapeutic effects of antibiotics using silkworms infected with human pathogenic microorganisms. Antimicrob. Agents Chemother. *48*, 774–779.

Han, Z.S., Enslen, H., Hu, X., Meng, X., Wu, I.H., Barrett, T., Davis, R.J., and Ip, Y.T. (1998). A conserved p38 mitogen-activated protein kinase pathway regulates *Drosophila* immunity gene expression. Mol. Cell. Biol. *18*, 3527–3579.

Hoffmann, J.A. (2003). The immune response of *Drosophila*. Nature *426*, 33–38.

Kanuka, H., Kuranaga, E., Takemoto, K., Hiratou, T., Okano, H., and Miura, M. (2005). Drosophila caspase transduces Shaggy/GSK-3beta kinase activity in neural precursor development. EMBO J. *24*, 3793–3806.

Kim, D.H., Feinbaum, R., Alloing, G., Emerson, F.E., Garsin, D.A., Inoue, H., Tanaka-Hino, M., Hisamoto, N., Matsumoto, K., Tan, M.W., and Ausubel, F.M. (2002). A conserved p38 MAP kinase pathway in *Caenorhabditis elegans* innate immunity. Science *297*, 623–626.

Kim, T., Yoon, J., Cho, H., Lee, W.B., Kim, J., Song, Y.H., Kim, S.N., Yoon, J.H., Kim-Ha, J., and Kim, Y.J. (2005). Downregulation of lipopolysaccharide response in *Drosophila* by negative crosstalk between the AP1 and NF-kappaB signaling modules. Nat. Immunol. *6*, 211–218.

Kover, P.X., and Schaal, B.A. (2002). Genetic variation for disease resistance and tolerance among *Arabidopsis thaliana* accessions. Proc. Natl. Acad. Sci. USA *99*, 11270–11274.

Kurucz, E., Markus, R., Zsamboki, J., Folkl-Medzihradszky, K., Darula, Z., Vilmos, P., Udvardy, A., Krausz, I., Lukacsovich, T., Gateff, E., et al. (2007). Nimrod, a putative phagocytosis receptor with EGF repeats in *Drosophila* plasmatocytes. Curr. Biol. *17*, 649–654.

Lemaitre, B., and Hoffmann, J.A. (2007). The host defense of *Drosophila melanogaster*. Annu. Rev. Immunol. *25*, 697–743.

Mansfield, B.E., Dionne, M.S., Schneider, D.S., and Freitag, N.E. (2003). Exploration of host-pathogen interactions using Listeria monocytogenes and *Drosophila melanogaster*. Cell. Microbiol. *5*, 901–911.

Miki, T., Okada, N., Shimada, Y., and Danbara, H. (2004). Characterization of Salmonella pathogenicity island 1 type III secretion-dependent hemolytic activity in *Salmonella enterica serovar* Typhimurium. Microb. Pathog. *37*, 65–72.

Nagai, H., and Roy, C.R. (2001). The DotA protein from *Legionella pneumophila* is secreted by a novel process that requires the Dot/Icm transporter. EMBO J. *20*, 5962–5970.

Raberg, L., Sim, D., and Read, A.F. (2007). Disentangling genetic variation for resistance and tolerance to infectious diseases in animals. Science *318*, 812–814.

Raupach, B., and Kaufmann, S.H. (2001). Immune responses to intracellular bacteria. Curr. Opin. Immunol. *13*, 417–428.

Rausher, M.D. (2001). Co-evolution and plant resistance to natural enemies. Nature *411*, 857–864.

Roy, B.A., and Kirchner, J.W. (2000). Evolutionary dynamics of pathogen resistance and tolerance. Evolution Int. J. Org. Evolution *54*, 51–63.

Sato, M., and Kornberg, T.B. (2002). FGF is an essential mitogen and chemoattractant for the air sacs of the drosophila tracheal system. Dev. Cell *3*, 195–207.

Schneider, D.S., and Ayres, J.S. (2008). Two ways to survive infection: what resistance and tolerance can teach us about treating infectious diseases. Nat. Rev. Immunol. *8*, 889–895.

Schneider, D.S., Ayres, J.S., Brandt, S.M., Costa, A., Dionne, M.S., Gordon, M.D., Mabery, E.M., Moule, M.G., Pham, L.N., and Shirasu-Hiza, M.M. (2007). *Drosophila eiger* mutants are sensitive to extracellular pathogens. PLoS Pathog. *3*, e41. 10.1371/journal.ppat.0030041.

Soderhall, K., and Cerenius, L. (1998). Role of the prophenoloxidase-activating system in invertebrate immunity. Curr. Opin. Immunol. *10*, 23–28.

Stramer, B., Wood, W., Galko, M.J., Redd, M.J., Jacinto, A., Parkhurst, S.M., and Martin, P. (2005). Live imaging of wound inflammation in *Drosophila* embryos reveals key roles for small GTPases during in vivo cell migration. J. Cell Biol. *168*, 567–573.

Toba, G., Ohsako, T., Miyata, N., Ohtsuka, T., Seong, K.H., and Aigaki, T. (1999). The gene search system. A method for efficient detection and rapid molecular identification of genes in *Drosophila melanogaster*. Genetics *151*, 725–737.

Valdivia, R.H., and Falkow, S. (1997). Fluorescence-based isolation of bacterial genes expressed within host cells. Science *277*, 2007–2011.

Zhuang, Z.H., Zhou, Y., Yu, M.C., Silverman, N., and Ge, B.X. (2006). Regulation of *Drosophila* p38 activation by specific MAP2 kinase and MAP3 kinase in response to different stimuli. Cell. Signal. *18*, 441–448.

Experimental Parasitology 125 (2010) 179–183

Contents lists available at ScienceDirect

Experimental Parasitology

journal homepage: www.elsevier.com/locate/yexpr

Research brief

A single fluorescence-based LAMP reaction for identifying multiple parasites in mosquitoes

Hiroka Aonuma [a,b], Aya Yoshimura [a], Tomomi Kobayashi [a], Kiyoshi Okado [a], Athanase Badolo [a,c], Bryce Nelson [a], Hirotaka Kanuka [a,*], Shinya Fukumoto [a,*]

[a] National Research Center for Protozoan Diseases, Obihiro University of Agriculture and Veterinary Medicine, Inada-cho, Obihiro, Hokkaido 080-8555, Japan
[b] Department of Parasitology, National Institute of Infectious Diseases, Shinjuku-ku, Tokyo 162-8640, Japan
[c] Centre National de Recherche et de Formation sur le Paludisme, Ouagadougou, Burkina Faso

ARTICLE INFO

Article history:
Received 18 August 2009
Received in revised form 17 November 2009
Accepted 24 December 2009
Available online 11 January 2010

Keywords:
Vector
LAMP
Diagnosis
Malaria
Filariasis

ABSTRACT

Vector-borne diseases, such as malaria and lymphatic filariasis, are co-endemic in large parts of the world. To develop a multiplex amplification method for the simultaneous detection of multiple insect-borne infectious diseases, we used LAMP with fluorescently labeled primers to identify the *SPECT2* gene of *Plasmodium berghei* and the *cytochrome oxidase subunit I* gene of *Dirofilaria immitis* in mosquitoes. This technique could detect as few as 100 *P. berghei*-infected red blood cell-equivalents or one *D. immitis* microfilaria. Moreover, individual species of parasites in mosquitoes could be identified when a mixture of fluorescently labeled primer sets was used. These findings suggest that the multiplex LAMP assay is sensitive and specific enough to identify parasite-bearing mosquitoes in areas where several diseases occur simultaneously. This procedure could increase the efficiency and effectiveness of arthropod-borne disease elimination programs.

1. Introduction

Mosquitoes are important arthropod vectors for various disease-causing pathogens, including parasites, bacteria, and viruses, that infect a variety of hosts, including humans. Many of these diseases continue to pose an endemic threat to human populations, despite the ongoing efforts of elimination programs, such as the Global Malaria Program and Global Program to Eliminate Lymphatic Filariasis, run by the World Health Organization (WHO) (WHO, 2008a,b). These programs were devised to attempt "comprehensive vector-borne disease control" (WHO, 1995), because several of these important diseases are co-endemic (Muturi et al., 2008; Chadee et al., 2003; Ravindran et al., 1998) and transmitted by the same arthropod genus (Chadee et al., 2003; Burkot et al., 1990a). Moreover, in the case of mosquito-borne illness, some species of mosquito can carry and transmit more than one pathogen (Albuquerque and Ham, 1995), and occasionally, individual mosquitoes have been shown carry two pathogens simultaneously (Muturi et al., 2006; Burkot et al., 1990b). Thus, a method for detecting multiple pathogens in a single reaction would make parasite surveys more efficient and effective.

To this end, we examined the applicability of fluorescence-based loop-mediated isothermal amplification (LAMP) for the detection of *Plasmodium berghei* and *Dirofilaria immitis* in mosquitoes. LAMP is a widely used DNA amplification method for carrying out reactions under isothermal conditions (Notomi et al., 2000) using a single enzyme; this method has a higher reaction specificity than conventional PCR methods (Mori et al., 2001).

Malaria and filariasis are debilitating parasitic infectious diseases transmitted by mosquito vectors that affect more than one million people worldwide (WHO, 2007a,b). We recently demonstrated the applicability of LAMP for detecting parasites in mosquitoes with high sensitivity: a single *P. berghei* oocyst could be detected in *Anopheles stephensi* and a single *D. immitis* worm in *Aedes aegypti* (Aonuma et al., 2008, 2009). Here we report the development of a fluorescence-based detection assay for the combined survey of both pathogens using the same reaction conditions.

2. Materials and methods

2.1. Preparation of parasites and infected mosquitoes

To evaluate the detection of malarial parasites using our method, infected red blood cells (iRBCs) were collected from 7- to 8-week-old BALB/c mice that had been infected with the rodent malaria *P. berghei* ANKA strain. This strain expresses GFP driven by the *hsp70* promoter, permitting the easy detection of infected

* Corresponding authors. Fax: +81 155 49 5643.
E-mail addresses: kanuka@obihiro.ac.jp (H. Kanuka), fukumoto@obihiro.ac.jp (S. Fukumoto).

0014-4894/$ - see front matter © 2010 Elsevier Inc. All rights reserved.
doi:10.1016/j.exppara.2009.12.023

cells (a gift from Dr. M. Yuda; Ishino et al., 2006). The blood was stored at −20 °C until needed for DNA extraction. Female vector mosquitoes of the strain *A. stephensi* were allowed to feed on anaesthetized infected mice, and were then kept at 19 °C until their dissection for microscopic analysis. To evaluate the efficiency of LAMP performed on oocyst-carrying mosquitoes, each mosquito midgut was dissected in ice-cold PBS, and the number of oocysts was counted under a microscope. Each midgut was then collected along with the remaining carcass, and the tissues were stored at −20 °C until needed for DNA extraction.

For the filarial parasite-transmission model, we used *D. immitis*, and the vector mosquito *Ae. aegypti*. To culture microfilariae, adult *D. immitis* worms were isolated from an infected dog and cultured in RPMI 1640 medium. The microfilariae were paralyzed by cooling at 4 °C and collected by centrifugation at 130g, for 10 min. The isolated microfilariae were counted with a cytometer and stored at −20 °C until needed. *Ae. aegypti* mosquitoes were fed *D. immitis*-infected blood by loading sheets of Parafilm (Pechiney Plastic Packaging, Inc., Illinois, USA) with infected dog blood, and attaching the blood-filled Parafilm to the bottom of a culture flask containing warm water. The membrane feeder was then placed over a netted mosquito cup for 1 h. The infected mosquitoes were kept at 27 °C until 8 days post-infection, to allow the *D. immitis* to reach the L2 stage. The Malpighian tubules were then dissected from the infected mosquitoes in ice-cold PBS, examined microscopically to count the number of parasites, and the entire carcass, including the Malpighian tubules and parasites, of each mosquito was stored −20 °C until needed for DNA extraction.

2.2. DNA extraction

The genomic DNA of *P. berghei* iRBCs, *D. immitis* microfilariae, and infected mosquitoes was extracted by homogenizing the cells or organisms with a plastic homogenizer in Buffer A (0.1 M Tris, pH 9.0; 0.1 M EDTA; 1% SDS; and 0.5% DEPC) and incubating the homogenate for 30 min at 70 °C. Next, 22.4 μl of 5 M KoAc was added, and the mixture was cooled for 30 min on ice. After centrifugation at 20,000g for 15 min at 4 °C, the DNA-containing supernatant was transferred to a new tube and mixed with 45 μl isopropanol. The solution was centrifuged at 20,000g for 20 min at 4 °C, and the precipitated DNA was collected, rinsed with 70% ethanol, and dried. Each DNA pellet was diluted in TE, and the final DNA concentrations per 1 μl were equal to 1×10^5 iRBCs, 1×10^4 microfilariae, or one-fifth of a mosquito. Finally, 1 μl of each DNA solution was used as a template for the LAMP reaction.

2.3. LAMP reactions

The loci and sequences of the primers (F3, B3, FIP, and BIP) were described previously (Aonuma et al., 2008, 2009). The FIP primers were labeled with either the FITC (*P. berghei*) or Cy5.5 (*D. immitis*) fluorescent dye (Fig. 1). The LAMP reaction was performed according to the manufacturer's instructions (Eiken Chemical Co., Ltd., Tokyo, Japan). Briefly, the 12.5 μl reaction mixture contained 1 μl of extracted DNA, 2.5 pmol of each F3 and B3 primer, 20 pmol of each FIP and BIP primer, 6.25 μl of 2× Reaction Mix, and 0.5 μl of *Bst* DNA polymerase. The reaction mixture was incubated at 60 °C for 90 min using a Loopamp Real-time Turbidimeter (LA-200; Eiken Chemical Co., Ltd., Tokyo, Japan). The reaction was terminated by incubation at 95 °C for 2 min.

2.4. Analysis of LAMP products

Amplified DNA in the LAMP reaction causes turbidity due to the accumulation of magnesium pyrophosphate, a by-product of the reaction. The turbidity was monitored using both a Loopamp Real time Turbidimeter (LA-200; Eiken Chemical Co., Ltd., Tokyo, Japan) and the naked eye. Each LAMP product was subjected to electrophoresis in a 2% agarose gel at 100 V, and the fluorescent dye-conjugated fragments were examined with an image analyzer (LAS-3000; Fujifilm Corporation, Tokyo, Japan) before the gels were stained with ethidium bromide for examination under UV light.

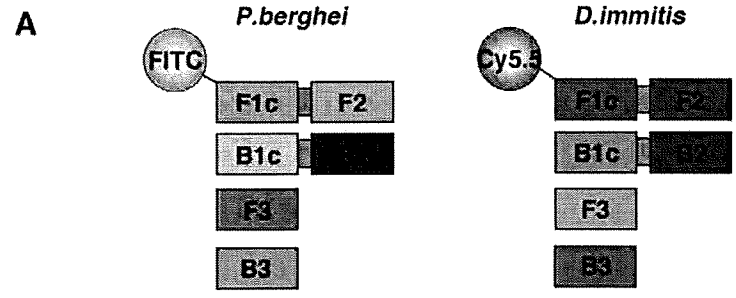

B

Primer	Sequence (5'→3')
P. berghei	
F3	ATGGGAAACTCAAACGACAA
B3	GGTGATTTTACGTATGGGCTG
FITC-FIP(F1c-F2)	CTGCACCATGGAAATCATCTTTTGCTACCTTGTGTGTGTTGATGC
BIP(B1c-B2)	GACGGGGAATTAGTTCTAAGTTGCCGTTTCCCCTGTAAATCCAGTT
D. immitis	
F3	CCTGTTTTGGCTGGTTCTT
B3	AGCAAAAGTCATACTAGTCTGG
Cy5.5-FIP(F1c-F2)	ACCTCAGGATGTCCAAAAAACCAAAATGATGCTAATAAGGGGGGTAA
BIP(B1c-B2)	TACCGGTGTTTGGGATTGTTAGTGCCAAACAAACGATCCTTATCAGTC

Fig. 1. LAMP primer sets targeting the *P. berghei SPECT2* and *D. immitis cytochrome oxidase subunit I* gene. (A) Primers designed for the fluorescence-based LAMP reaction. FIP primers were conjugated with the fluorescent dye FITC (*P. berghei*) or Cy5.5 (*D. immitis*). (B) Sequences of primers used in the LAMP reactions.

3. Results and discussion

The sensitivity and specificity of LAMP reactions containing primer sets for both pathogens, including the fluorescent dye-labeled primers, were examined in reactions with *P. berghei* DNA equivalent to 1×10^0, 1×10^1, 1×10^2, and 1×10^3 iRBCs or *D. immitis* DNA equivalent to $1x10^0$, $1x10^1$, $1x10^2$, and $1x10^3$ microfilariae, as templates. Consistent with previous results (Aonuma et al., 2008, 2009) the LAMP reaction was sensitive enough to detect single parasite of *D. immitis*, albeit at slightly longer reaction times, suggesting that the conjugation of fluorescent dyes to the primers did not appreciably inhibit this LAMP reaction (Fig. 2A). The sensi-

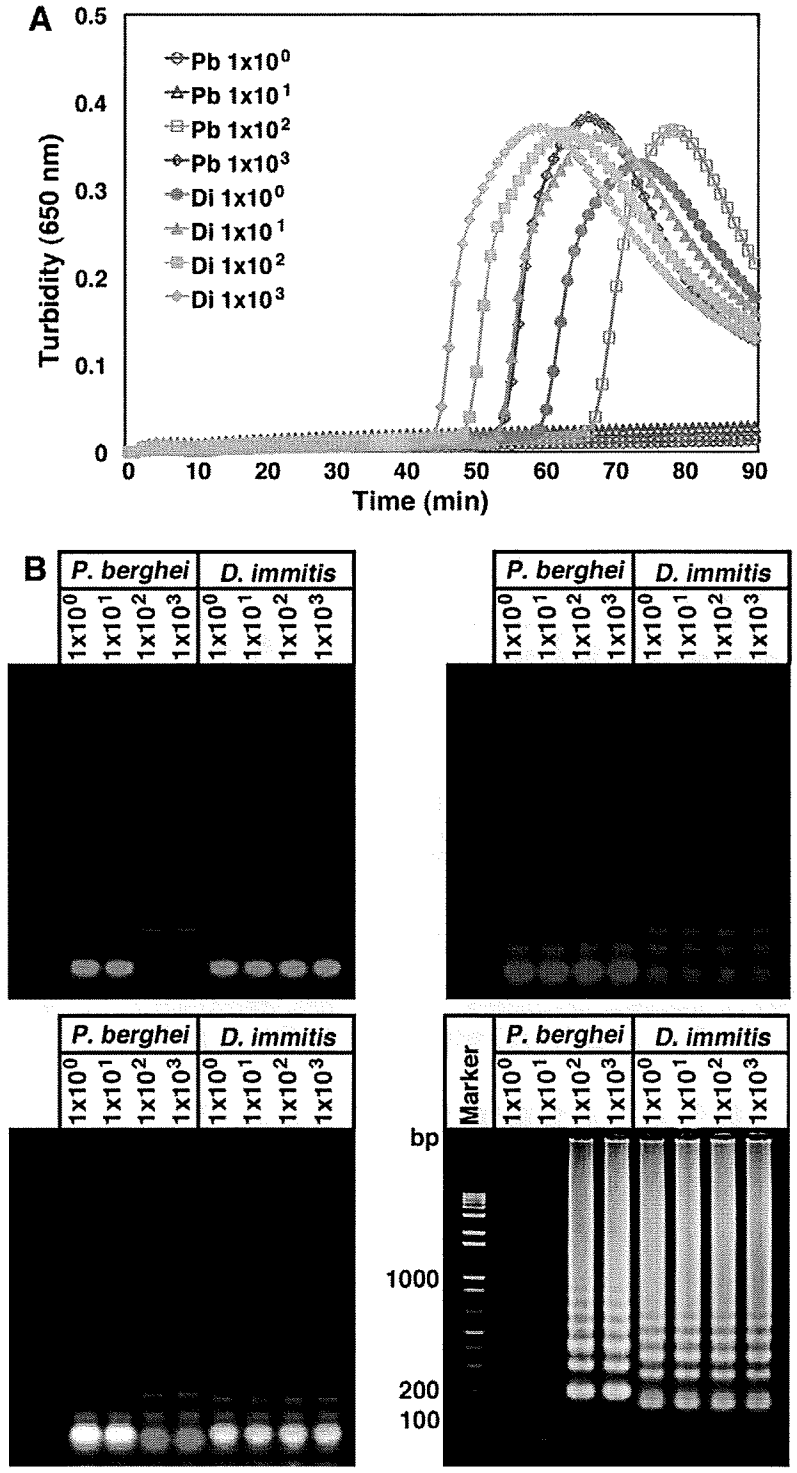

Fig. 2. Sensitivity of fluorescence-based LAMP detection of *P. berghei* and *D. immitis*. (A) Amplification of the target sequence with a primer set monitored by real-time turbidimeter (turbidity at 650 nm). *P. berghei* DNA (equivalent to 1×10^0, 1×10^1, 1×10^2, or 1×10^3 iRBCs) or *D. immitis* DNA (equivalent to 1×10^0, 1×10^1, 1×10^2, and 1×10^3 microfilariae) were used as templates for LAMP reactions of 90 min at 60 °C. (B) Agarose-gel electrophoresis of the LAMP-amplified products from (A). FITC fluorescence (green) indicates the amplified DNA sequence from *P. berghei* and Cy5.5 fluorescence (magenta) indicates that from *D. immitis* microfilariae. FITC (upper left), Cy5.5 (upper right), FITC and Cy5.5 merged image (left below), and ethidium bromide (right below). Numbers at left indicate the migration of molecular weight markers (bp).

tivity of *P. berghei* detection was slightly reduced, but low levels of parasitic load could still be detected. The optimized conditions were 60 °C for 90 min (data not shown). Using the optimized conditions, we next tested whether multiplex LAMP could be used to detect *P. berghei* or *D. immitis* simultaneously under the same reaction conditions. Both the FITC-labeled and Cy5.5-labeled primer sets were included in the reaction mixtures with DNA from either *P. berghei* or *D. immitis*. The fluorescence analysis of the amplified DNA demonstrated that each primer set specifically amplified the DNA of *P. berghei* (FITC) or *D. immitis* (Cy5.5) (Fig. 2B) under the same reaction conditions (Fig. 2B), indicating that LAMP performed using fluorescent dye-conjugated primers might enable the identification of two different parasitic species at the same time.

To evaluate the feasibility of a combined LAMP method designed to survey pathogen-carrying mosquitoes, we examined mosquitoes carrying *Plasmodium* or *Dirofilaria*. *A. stephensi* and *Ae. aegypti* were dissected, and the *P. berghei* oocysts and *D. immitis* second-stage larvae (L2), respectively, were counted. The number

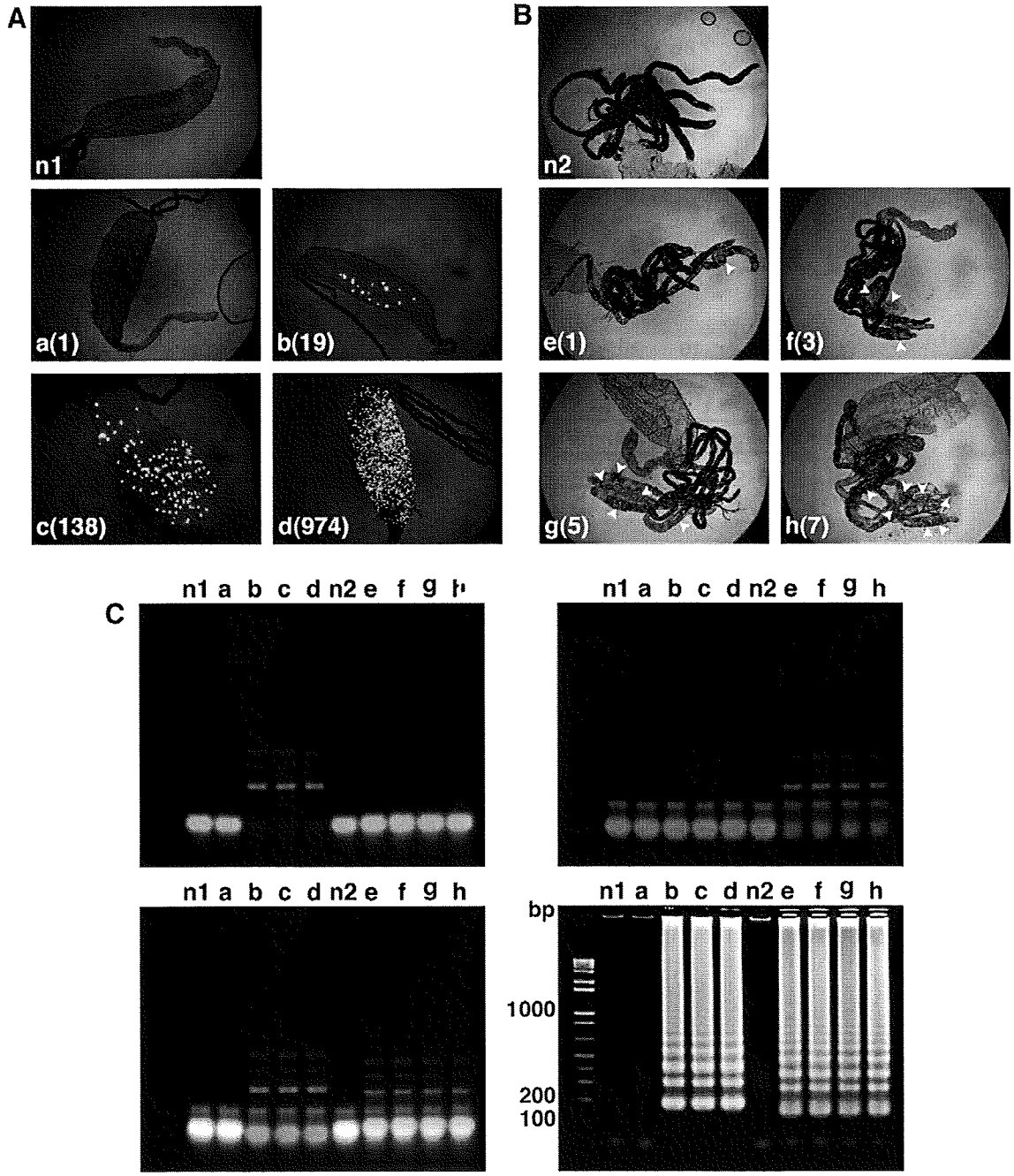

Fig. 3. LAMP-based identification of *P. berghei*- and *D. immitis*-carrying mosquitoes. (A) Each *P. berghei*-positive mosquito was observed under fluorescence microscopy to determine its state of infection. The punctate GFP signals (green spots) indicate *P. berghei* oocysts in the mosquito midgut (a–d). The number of oocysts is given in parenthesis. The uninfected mosquito shown in (n1) was used as a negative control. (B) Each *D. immitis*-carrying mosquito was observed under a microscope to determine its state of infection. Each white arrowhead indicates a *D. immitis* L2 larva in the mosquito Malpighian tubules (e–h). The number of L2 larvae is given in parenthesis. The Malpighian tubules of the uninfected mosquito shown in (n2) were used as a negative control. (C) LAMP detection of *P. berghei* oocysts and *D. immitis* L2 larvae in mosquitoes. Agarose-gel electrophoresis of the LAMP-amplified products from the samples in (A) and (B). FITC fluorescence (green) indicates *P. berghei* and Cy5.5 fluorescence (magenta) indicates *D. immitis* DNA. FITC (upper left), Cy5.5 (upper right), FITC and Cy5.5 merged image (left below), and ethidium bromide (right below). Numbers at left indicate the migration of molecular weight markers (bp).

of *P. berghei* oocysts per mosquito ranged from 1 to 974, and the *D. immitis* L2 larvae numbered between 1 and 7 (Fig. 3A and B). Next, the genomic DNA from each mosquito, along with the dissected midgut or malpighian tubules, was extracted and used for LAMP reactions. Notably, even small numbers of parasites, such as 1 *D. immitis* L2 larva or 19 *P. berghei* oocysts, could be detected in a single LAMP reaction tube containing the DNA of either parasite, but both sets of fluorescent dye-conjugated primers (Fig 3C).

The high sensitivity of the combined LAMP reaction, as demonstrated by the detection of a single parasite, was similar to that of individual LAMP reactions, demonstrated previously (Aonuma et al., 2008, 2009). Although the detection limit for *P. berghei* DNA in this study was limited to the equivalent of 50 iRBCs (data not shown), which is higher than in previous reports, infected mosquitoes contain thousands of sporozoites in their salivary glands. Therefore, this method is more than sufficiently sensitive for identifying infectious mosquitoes in the wild.

Our evaluation demonstrated that the LAMP procedure for detecting two different parasite species under the same reaction conditions was applicable for the identification of pathogen-carrying mosquitoes. Recently, several reports have shown that some species of mosquitoes act as vectors for both malarial and filarial parasites, sometimes carrying both pathogens at the same time. For example, *A. gambiae* is a potential vector for both *P. falciparum* and *Wuchereria bancrofti*, and occasionally an individual mosquito carries and transmits both parasites simultaneously (Muturi et al., 2006; Burkot et al., 1990b). We did attempt during this study to detect *P. berghei* and *D. immitis* simultaneously by LAMP in one reaction tube. However, the signals were poor, presumably due to some conflict in the enzymatic reactions (data not shown). We regard this study as a first step in the development of the new method for multiplex LAMP, and further investigation is needed to find the appropriate conditions for the synchronous LAMP reactions. Nonetheless, since the endemic areas for these two diseases largely overlap, the method developed in this study is expected to improve the effectiveness and efficiency of parasite surveys.

In this study, we demonstrated the utility of the multiplex LAMP method using fluorophore-conjugated primers to identify parasites in mosquitoes accurately and specifically. While *P. berghei* and *D. immitis* were used as model parasites in this study, this method should be easily amended for the diagnosis of other arthropod-borne parasitic diseases in humans, such as *P. falciparum*, *W. bancrofti*, and *Brugia malayi*. This method offers the possibility of a combined survey of multiple infectious diseases in areas where such diseases are co-endemic, thereby reducing the cost and time of diagnosis. Furthermore, the successful identification of infected mosquitoes using multiplex LAMP indicates that this method could provide a more efficient means to analyze the disease status of mosquitoes collected from field surveys.

Acknowledgments

We thank Tomoko Ishino, Masao Yuda, and Yasuo Chinzei for the malaria strain and *Anopheles* mosquito, Hiroshi Iseki for the primer design, and Kazutaka Yamada and Ryu-ichiro Maeda for the filaria and *Aedes* mosquito. We are also grateful to Yukari Furukawa, Emi Maekawa, Yuko Doi, Chisako Kashima, Hironori Bando, Kazuhiro Bandai, and Tokiyasu Teramoto for mosquito rearing, and Oriel Thekisoe for valuable discussion. This study was supported in part by grants from the Health Sciences Research Grant for Research on Emerging and Re-emerging Infectious Diseases from the Ministry of Health, Labor, and Welfare to H.K. and S.F., Grants-in-Aid for Scientific Research from the Japanese Ministry of Education, Science, Sports, Culture and Technology to H.K. and S.F., and the Program for the Promotion of Basic Research Activities for Innovative Biosciences (PROBRAIN) to H.K. B.N. is a research fellow of the Japan Society for the Promotion of Science.

References

Albuquerque, C.M., Ham, P.J., 1995. Concomitant malaria (*Plasmodium gallinaceum*) and filaria (*Brugia pahangi*) infections in *Aedes aegypti*: effect on parasite development. Parasitology 110, 1–6.

Aonuma, H., Suzuki, M., Iseki, H., Perera, N., Nelson, B., Igarashi, I., Yagi, T., Kanuka, H., Fukumoto, S., 2008. Rapid identification of *Plasmodium*-carrying mosquitoes using loop-mediated isothermal amplification. Biochemical and Biophysical Research Communications 376, 671–676.

Aonuma, H., Yoshimura, A., Perera, N., Shinzawa, N., Bando, H., Oshiro, S., Nelson, B., Fukumoto, S., Kanuka, H., 2009. Loop-mediated isothermal amplification applied to filarial parasites detection in the mosquito vectors: *Dirofilaria immitis* as a study model. Parasites and Vectors 2, 15.

Burkot, T.R., Garner, P., Paru, R., Dagoro, H., Barnes, A., McDougall, S., Wirtz, R.A., Campbell, G., Spark, R., 1990a. Effect of untreated bed nets on the transmission of *Plasmodium falciparum*, *P. Vivax* and *Wuchereria bancrofti* in Papua New Guinea. Transactions of the Royal Society of Tropical Medicine and Hygiene 84, 773–779.

Burkot, T.R., Molineaux, L., Graves, P.M., Paru, R., Battistutta, D., Dagoro, H., Barnes, A., Wirtz, R.A., Garner, P., 1990b. The prevalence of naturally acquired multiple infections of *Wuchereria bancrofti* and human malarias in anophelines. Parasitology 100, 369–375.

Chadee, D.D., Rawlins, S.C., Tiwari, T.S., 2003. Short communication: concomitant malaria and filariasis infections in Georgetown, Guyana. Tropical Medicine and International Health 8, 140–143.

Ishino, T., Orito, Y., Chinzei, Y., Yuda, M., 2006. A calcium-dependent protein kinase regulates *Plasmodium* ookinete access to the midgut epithelial cell. Molecular Microbiology 59, 1175–1184.

Mori, Y., Nagamine, K., Tomita, N., Notomi, T., 2001. Detection of loop-mediated isothermal amplification reaction by turbidity derived from magnesium pyrophosphate formation. Biochemical and Biophysical Research Communications 289, 150–154.

Muturi, E.J., Mbogo, C.M., Mwangangi, J.M., Ng'ang'a, Z.W., Kabiru, E.W., Mwandawiro, C., Beier, J.C., 2006. Concomitant infections of *Plasmodium falciparum* and *Wuchereria bancrofti* on the Kenyan coast. Filaria Journal 5, 8.

Muturi, E.J., Jacob, B.G., Kim, C.H., Mbogo, C.M., Novak, R.J., 2008. Are coinfections of malaria and filariasis of any epidemiological significance? Parasitology Research 102, 175–181.

Notomi, T., Okayama, H., Masubuchi, H., Yonekawa, T., Watanabe, K., Amino, N., Hase, T., 2000. Loop-mediated isothermal amplification of DNA. Nucleic Acids Research 28, E63.

Ravindran, B., Sahoo, P.K., Dash, A.P., 1998. Lymphatic filariasis and malaria: concomitant parasitism in Orissa, India. Transactions of the Royal Society of Tropical Medicine and Hygiene 92, 21–23.

World Health Organization, 1995. Vector control for Malaria and other mosquito-borne diseases. WHO Technical Report Series 857.

World Health Organization, 2007a. Fact sheet No. 94. WHO.

World Health Organization, 2007b. Weekly epidemiological record No. 42. WHO.

World Health Organization, 2008a. World malaria report. WHO.

World Health Organization, 2008b. Weekly epidemiological record. WHO 83, 333–348.

Am. J. Trop. Med. Hyg., 82(5), 2010, pp. 855–860
doi:10.4269/ajtmh.2010.09-0533

Detection of *Trypanosoma cruzi* and *T. rangeli* Infections from *Rhodnius pallescens* Bugs by Loop-Mediated Isothermal Amplification (LAMP)

Oriel M. M. Thekisoe, Carol V. Rodriguez, Francisco Rivas, Andrea M. Coronel-Servian, Shinya Fukumoto, Chihiro Sugimoto, Shin-Ichiro Kawazu, and Noboru Inoue*

National Research Center for Protozoan Diseases, Obihiro University of Agriculture and Veterinary Medicine, Obihiro, Japan; College of Medicine, Department of Microbiology, University of Panamá, Panama; Research Center for Zoonosis Control, Hokkaido University, Sapporo, Japan

Abstract. We have developed two loop-mediated isothermal amplification (LAMP) assays for specific detection of *Trypanosoma cruzi* and *Trypanosoma rangeli* based on the 18S ribosomal RNA (rRNA) and the small nucleolar RNA (snoRNA) genes, respectively. The detection limit of the assays is 100 fg and 1 pg for *T. cruzi* and *T. rangeli*, respectively, with reactions conducted in 60 minutes. The two LAMP assays were used in detection of *T. cruzi* and *T. rangeli* infections in comparison with polymerase chain reaction (PCR) for DNA samples extracted from *Rhodnius pallescens* bugs collected from palm trees in Panama. Out of a total of 52 DNA samples from *R. pallescens* bugs 17 (33%) and 14 (27%) were *T. cruzi*-positive by LAMP and PCR, respectively, while, 7 (13%) and 4 (8%) were *T. rangeli*-positive by LAMP and PCR, respectively. Further evaluation of these LAMP assays is needed, especially with specimens collected from human patients as well as blood kept for transfusion purposes.

INTRODUCTION

Trypanosoma cruzi infects human beings and causes Chagas disease/American trypanosomiasis in Central and South America. It is transmitted by *Rhodnius* and *Triatoma* bugs through contaminated feces,[1,2] and can also be transmitted vertically by blood transfusion or during organ transplantation.[3] The non-pathogenic *Trypanosoma rangeli* shares the same geographical location and same insect vectors with *T. cruzi*,[2,4,5] hence, necessitating accurate differential diagnosis. *Trypanosoma rangeli* is capable of transmission both through feces and through the salivary glands.[6] Diagnosis of American trypanosomiasis relies on serological techniques, primarily using an indirect immunofluorescence assay (IFA) with *T. cruzi* epimastigote forms.[4] Xenodiagnosis is mainly used for direct detection of *T. cruzi* parasites, although sometimes it is not effective in patients with very low parasitaemia,[7] and furthermore, it is time consuming. Polymerase chain reaction (PCR) allows precise identification of the infecting trypanosome species from blood or tissue samples, and detection of trypanosomes in the vectors.[2,5,7] Despite its high specificity and sensitivity, the use of PCR is still not widespread in diagnostic laboratories of endemic areas,[4] mainly because of high costs and the requirement for specialized equipment.[8,9]

The loop-mediated isothermal amplification (LAMP) method is a gene amplification technique that uses 4 or 6 primers that detect DNA of pathogenic organisms with high sensitivity and specificity.[10,11] The major advantages of LAMP include: 1) the reaction is isothermal and detection can be conducted within 60 minutes, 2) it requires simple heating devices such as a water bath or laboratory heat block, and 3) the detection of reaction results can be seen immediately after incubation by the naked eye caused by turbidity occurring in positive amplification reactions[12] or by addition of fluorescent dyes after incubation such as SYBR green, ethidium bromide, or evagreen, which enable detection under UV light.[13] A more convenient loopamp fluorescent detection reagent (FD) (Eiken Chemical Co. Ltd., Tokyo, Japan) has been specifically developed for detection of LAMP products, whereby its addition to the reaction mixture before incubation enables detection of results immediately after incubation by the naked eye under UV without opening the reaction tube.[14] We have previously reported on LAMP primers developed for detection of *T. cruzi* infections,[15] although they were never tested with field samples from infected hosts or vectors. In this study, we have developed LAMP assays for detection of *T. cruzi* and *T. rangeli* by targeting the 18S ribosomal RNA (rRNA) and small nucleolar RNA (snoRNA) genes, respectively, and further used these assays for detection of *T. cruzi* and *T. rangeli* infections in triatomine bugs collected from royal palm trees (*Attalea butyracea*) in Viento Fronco, Chilibre district, Panama.

MATERIALS AND METHODS

Insect collection and DNA extraction. Fifty-two triatomine bugs were collected from royal palm trees (*Attalea butyracea*) growing nearby households in the community of Viento Fronco, Chilibre district, Colón province, Republic of Panamá. The bugs were transported to the laboratory with the permission of the Autoridad Nacional del Medio Ambiente (ANAM) from April to May 2006. In the laboratory the bugs were identified taxonomically and then dissected aseptically, and DNA was extracted from insect extracts (all internal organs of the bug) using the Puregene DNA Purification kit (Gentra Systems Inc., Minneapolis MN) according to the manufacturer's instructions. Briefly, cell lysis solution and proteinase K (100 μg/mL) were added to whole insect extracts. The mixture was pipetted up and down to lyse the cells and then incubated at 55°C overnight. Samples were cooled at room temperature, protein precipitation solution was added, and the mixture was then centrifuged. The DNA was finally precipitated with 100% isopropanol, washed with 70% ethanol, and then hydrated with 50 μL of DNA hydration solution.

For optimization, specificity, and sensitivity of the reactions, the phenol-chloroform method, as described by Sambrook and Russel,[16] was used for DNA extraction of *T. cruzi* (Tulahuan strain) epimastigotes from *in vitro* cultures and *Triatoma infestans* and *Rhodnius prolixus* from pathogen-free colonies of the National Research Center for Protozoan Diseases,

* Address correspondence to Noboru Inoue, National Research Center for Protozoan Diseases, Obihiro University of Agriculture and Veterinary Medicine, Inada-cho, Obihiro, Hokkaido 080-8555, Japan. E-mail: ircpmi@obihiro.ac.jp

Obihiro University and uninfected human blood DNA. The *T. rangeli* (Panama strain) DNA was kindly provided by Azael Saldaña, Parasitology Unit, College of Medicine, University of Panamá.

LAMP. Table 1 shows LAMP primer sets for *T. cruzi* and *T. rangeli* parasites targeting the 18S rRNA and the snoRNA-c11 genes, respectively, designed using the LAMP primer explorer software version 4 (http://primerexplorer.jp/e/). The LAMP reactions were performed as previously described by Notomi and others.[11] Briefly, a total volume of 25 μL containing 12.5 μL of 2× LAMP buffer (40 mM Tris-HCl [pH 8.8], 20 mM KCl, 16 mM $MgSO_4$, 20 mM $[NH_4]_2SO_4$, 0.2% Tween 20, 1.6 M Betaine, 2.8 mM of each deoxyribonucleotide triphosphates (dNTPs)), 1.3 μL primer mix (5 pmol each of F3 and B3, 40 pmol each of FIP and BIP and 20 pmol each of LF and LB), 8.2 μL distilled water, 1 μL (8 units) *Bst* DNA polymerase (New England Biolabs, Tokyo, Japan), and 2 μL of template DNA. In reactions whereby 1 μL FD was added to enable the detection by the naked eye, the volume of distilled water was adjusted appropriately. The reaction mixture was incubated at 63°C for 60 min using a Loopamp real-time turbidimeter (LA200, Teramecs, Tokyo, Japan).

PCR. The PCR reactions were performed with specific *T. cruzi* primers and *T. rangeli* primers reported previously.[17] The primer sequences are as follows:

For *T. cruzi*, Tcru1: 5′-AAA TAA TGT ACG GGK GAG ATG CAT GA-3′ and Tcru2: 5′-GGT TCG ATT GGG GTT GGT GTA ATA TA-3′ and for *T. rangeli*, TrINT1: 5′-CGC CCA TTC GTT TGT CC-3′ and TrINT2: 5′-TCC AGC GCC ATC ACT GAT C-3′. The PCR mixture (25 μL total volume) contained PCR Buffer (10 mM Tris-HCl [pH 8.3], 50 mM KCl, 1.5 mM $MgCl_2$), 2 mM each of the dNTPs, 5 pmol of each primer, and 0.5 U of AmpliTaq Gold DNA polymerase (Applied Biosystems, Japan). The reaction mixtures were incubated in a PCR thermocycler (Applied Biosystems, Singapore) at 94°C for 10 min (initial denaturation step), and then subjected to 35 cycles consisting of 45 s at 94°C (denaturation step), 1 min at 58°C (annealing step), and 1 min at 72°C (extension), followed by terminal elongation for 7 min at 72°C. The PCR products were electrophoresed in a 1.5% agarose gel and stained with ethidium bromide solution for visualization under UV light.

RESULTS AND DISCUSSION

The loopamp real-time turbidimetry device enables observation of primer kinetics. Therefore, at the commencement of the study, LAMP reactions were conducted at 60, 63, 65, and 67°C to determine the optimal reaction temperature for both the *T. cruzi* and *T. rangeli* primer sets. The temperature at which the reaction would reach and cross the positive reaction threshold, which is 0.1 of released turbidity[18] in a short period of time or faster than others, was selected as the optimal reaction temperature (these reactions were done in five repetitions). As a result, the 63°C temperature was chosen as the optimal reaction temperature because the reaction threshold time for positive reactions was achieved faster at this temperature (data not shown). The *T. cruzi* 18S LAMP assay specifically amplified *T. cruzi* DNA without amplifying negative control DNA of *T. rangeli*, vector insects, and human host (Figure 1A). The detection limit of the assay was 100 fg of serially diluted *T. cruzi* DNA (Figure 1B and C). The *T. rangeli* snoRNA LAMP assay also specifically amplified *T. rangeli* DNA without amplifying the negative control DNA (Figure 2A) with a detection limit of 1 pg as determined from serially diluted DNA (Figure 2B and C). In this study, six LAMP primers were used for amplification of each target trypanosome DNA. In this way eight distinct regions were recognized on the target gene, thereby ensuring specificity, high sensitivity, and rapid reaction whereby amplification is achieved within 60 minutes.[10]

Rhodnius pallescens is considered to be the most important and widespread vector of *T. cruzi* and *T. rangeli* in Panama.[19] In the current study, we therefore evaluated detection performance of the newly developed *T. cruzi* and *T. rangeli* LAMP assays on DNA extracted from triatomine bugs (37 nymphae and 15 adults) collected from palm trees in Panama. Of the 37 DNA samples extracted from *R. pallescens* nymphae, 10 (27%) and 7 (19%) were *T. cruzi*-positive by LAMP and PCR, respectively. Of the 15 adult *R. pallescens* DNA samples, 7 (47%) were positive for *T. cruzi* infections by both LAMP and PCR assays (Table 2). Therefore, out of a total of 52 DNA samples from *R. pallescens*, 17 (33%) and 14 (27%) were *T. cruzi*-positive by LAMP and PCR, respectively.

However, for *T. rangeli*, 3/37 (8%) were positively detected by LAMP from *R. pallescens* nymphae DNA, while none were positive by PCR. Of the 15 adult *R. pallescens* DNA samples, 4/15 (27%) were positively detected for *T. rangeli* infections by both LAMP and PCR (Table 2). Therefore, out of a total of 52 DNA samples from *R. pallescens*, 7 (13%) and 4 (8%) were *T. rangeli*-positive by LAMP and PCR, respectively. The LAMP assays developed in this study have shown a slightly higher detection performance than PCR. This is in agreement with previous studies where LAMP and PCR were compared

TABLE 1
LAMP primer sets used in this study

Species	Accession no.	Size of target	Gene	Primer sequence
Trypanosoma cruzi	AF301912	187 bp	FIP:	5′-CGTGAGTTGAGGGAAGGCATGAGTTGTTGGCAGACTTCGGT-3′
			BIP:	5′-GCATCCAGGAATGAAGGAGGGTTCGTCTTGGTGCGGTCTA-3′
			F3:	5′-CCGTGTGGCACTGTTTGT-3′
			B3:	5′-TGAAGAATGCCTTCGCTGT-3′
			LF:	5′-CATGTGAGATGCGAAGGG-3′
			LB:	5′-CATGTGAGATGCGAAGGG-3′
Trypanosoma rangeli	AY028385	172 bp	FIP:	5′-TCATGCGTCGCAGCCGTACGCGAGAACGGGAGCA-3′
			BIP:	5′-TTGCAGTTTCCTGTCAGCCTGACGTTTCAGTGTGAGCTGAGT-3′
			F3:	5′-CGAGGACGGGCGAGAA-3′
			B3:	5′-AAAAGGGGGGAAAGCAAGT-3′
			LF:	5′-CCCGCCTTCTTCGCTCT-3′
			LB:	5′-GCGCGTGACGACACAAC-3′

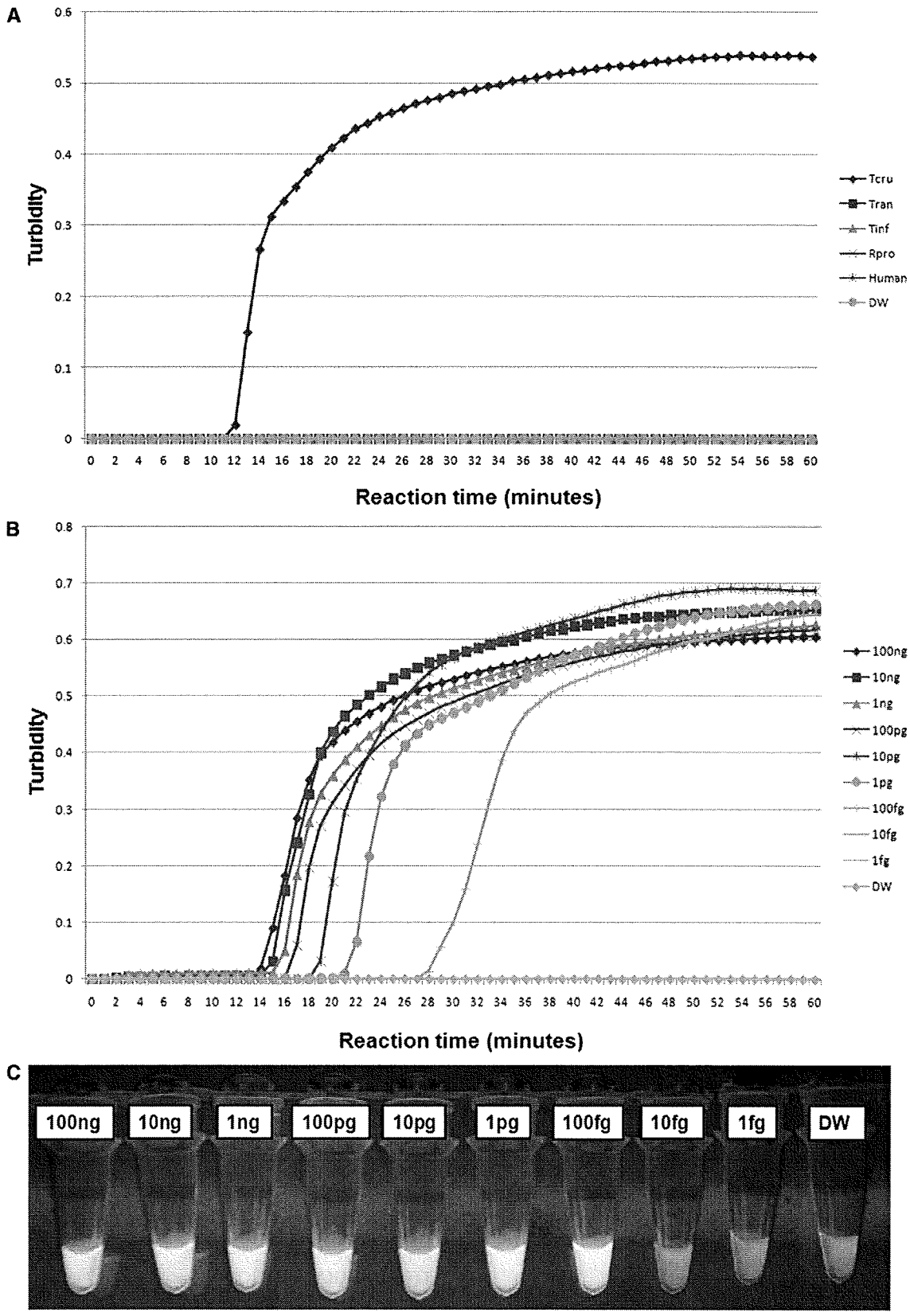

FIGURE 1. Loop-mediated isothermal amplification (LAMP) reactions with the 18S rRNA primer set for amplification of *Trypanosoma cruzi* DNA. Standard positive reaction threshold is 0.1 of the value of the turbidity released. (**A**) Specificity test of the LAMP assay using the real-time turbidimetry device. Tcru – *T. cruzi*; Tran – *Trypanosoma rangeli*; Tinf – *Triatoma infestans*; Rpro – *Rhodnius prolixus*; Human – DNA extracted from uninfected human blood; and DW – distilled water used as non-DNA negative control. Sensitivity test on serially diluted *T. cruzi* DNA from 100 ng down to 1 fg: (**B**) detection using the real-time turbidimetry device, (**C**) detection under UV light by the naked eye using FD reagent. The green/bright fluorescence indicates a positive reaction and the dark/less fluorescent color indicates a negative reaction. This figure appears in color at www.ajtmh.org.

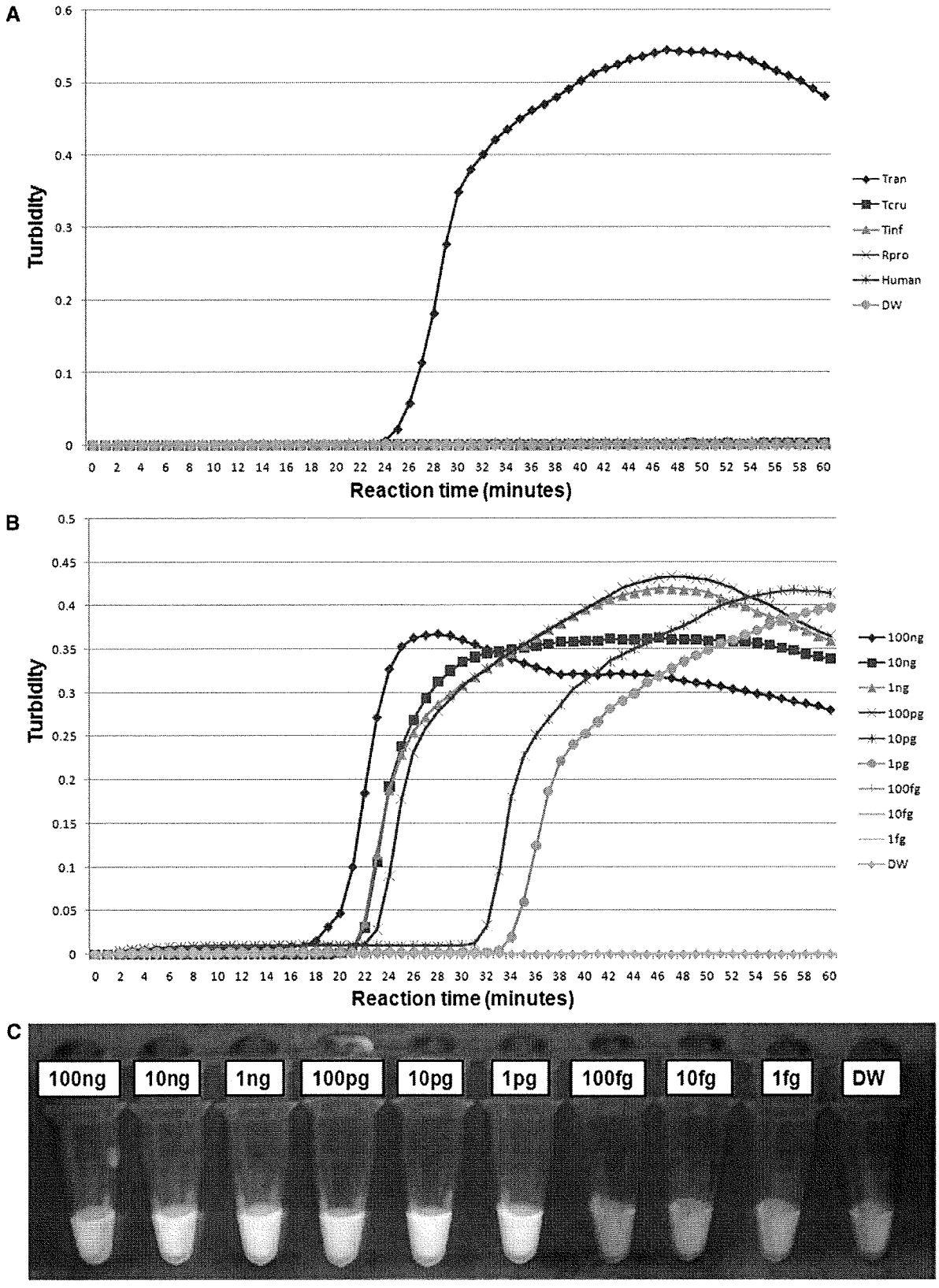

FIGURE 2. Loop-mediated isothermal amplification (LAMP) reactions with the snoRNA primer set for amplification of *Trypanosoma rangeli* DNA. Standard positive reaction threshold is 0.1 of the value of the turbidity released. (**A**) Specificity test of LAMP assay using the real-time turbidimetry device. Tran – *T. rangeli*; Tcru – *Trypanosoma cruzi*; Tinf – *Triatoma infestans*; Rpro – *Rhodnius prolixus*; Human – DNA extracted from uninfected human blood; and DW – distilled water used as non-DNA negative control. Sensitivity test on serially diluted *T. rangeli* DNA from 100 ng down to 1 fg: (**B**) detection using the real-time turbidimetry device, (**C**) detection under UV light by the naked eye using FD reagent. The green/bright fluorescence indicates a positive reaction and the dark/less fluorescent color indicates a negative reaction. This figure appears in color at www.ajtmh.org.